Optically pumped atoms with velocity- and spin-changing collisions at low gas pressures

Steven W. Morgan and William Happer
Princeton University Department of Physics, Princeton, New Jersey 08544, USA
(Received 20 August 2009; published 5 April 2010)

We discuss optical pumping when (a) the collision rates of optically pumped atoms with atoms or molecules of the background gas are small enough that individual velocity groups can be preferentially excited by a monochromatic light beam, (b) the collision rates are still fast enough to partially transfer the spin polarization to other velocity groups, and (c) there are nonnegligible losses of polarization due to collisional spin relaxation and Larmor precession. These conditions lead to a strong correlation between the velocity and the spin polarization of the atoms—that is, to "spin-tagging" of the different velocity groups. This regime is similar to that of optically pumped ^{23}Na atoms of the Earth's upper atmosphere, but it is seldom encountered in laboratory experiments. For cooling and trapping experiments, the collision rates with background gas are negligible. For gas-cell experiments the velocity-changing rates are normally so fast compared to spin relaxation or Larmor precession rates that the atoms have a Maxwellian velocity distribution with negligible correlation between the spin polarization and the velocity. We analyze the limiting cases of strong and weak collisions, which change the velocity by a large or small fraction, respectively, of the mean thermal velocity. The Keilson-Storer model [J. Keilson and A. E. Storer, Q. Appl. Math. **10**, 243 (1952)] is used to discuss strong collisions, with memory parameter $\alpha = 0$ and weak collisions with $\alpha \to 1$. For weak collisions, the physics can be modeled by coupled Fokker-Planck equations, identical to those for forced diffusion in a harmonic-oscillator potential well. In this limit there are solutions analogous to the quantum mechanical coherent states of a harmonic oscillator.

DOI: 10.1103/PhysRevA.81.042703 PACS number(s): 32.80.Xx, 02.30.Hq, 95.75.Qr, 05.20.Dd

I. INTRODUCTION

There has been increasing interest in the use of Na guidestars [1–5] in the adaptive optics community. A ground-based laser is tuned to the 590 nm D_2 line of Na atoms and directed toward the star or other astronomical object of interest. The laser scatters from the Na atoms that occur naturally in the atmosphere at an altitude of 90 to 100 km. The back scattered light from these atoms serves as an artificial star that can be used to compensate for atmospheric turbulence and to substantially improve the angular resolution of the telescope.

The lasers used to produce Na guidestars can cause optical pumping of the Na atoms. The number density $[N]$ of atmospheric molecules and atoms is so low [1], typically $[N] \approx 10^{14}$ cm^{-3}, that the optical absorption lines are almost those of collision-free atoms. This homogeneous linewidth is so narrow that only the small fraction of atoms that happen to have the resonant Doppler shift can interact with a monochromatic pumping laser. Velocity-changing collisions allow spin-polarized atoms produced at the resonant velocity to populate the rest of velocity space. Spin precession around the geomagnetic field, with a magnitude $B \approx 1/2$ gauss, is fast enough to substantially degrade any transverse spin polarization produced by the optical pumping in the time it takes for velocity-changing collisions to fill out the Maxwellian velocity distribution. The geomagnetic field does not matter if it happens to be parallel to the viewing direction, but it can be an important factor if it is nearly perpendicular to the viewing direction. Spin-flipping collisions with the "buffer gas" can also degrade the spin polarization before an atom can be transferred from the pumped velocity group to other velocity groups. A grazing-incidence collision between an alkali-metal atom and an O_2 molecule or O atom that causes a negligible change in velocity can be expected to flip the spin of the alkali-metal atom because of the large (basically electrostatic) exchange interaction between the unpaired electrons. This is similar to spin-exchange collisions between pairs of alkali-metal atoms in a laboratory environment, but the density [Na] $\approx 10^3$ cm^{-3} of Na atoms is so low in the upper atmosphere that collisions between pairs of Na atoms are completely negligible. In contrast, conventional laboratory buffer gases like N_2, He, or Ar do not have unpaired electron spins, so an alkali-metal atom can have a million or more velocity-changing collisions before the weak spin-rotation interaction [6] finally flips the spin. The conditions we summarized cause the optical pumping of the Na layer to be very different from that encountered in laboratory pumping of gas cells. The most striking difference will be a strong correlation between the spin polarization and the component of the atomic velocity along the laser beam. A close analog of the physics of the Na guidestar is encountered for optically pumped ^{154}Sm [7]. Here the nonspherically symmetric ground state has spin-relaxation rates comparable to the rates of velocity-changing collisions, even for buffer gases like N_2, He, Ne, Ar, Kr, and Xe that cause very slow spin relaxation for alkali-metal atoms.

Special mathematical tools are needed to analyze the physics discussed previously. We can model the behavior of the pumped atoms with evolution equations of the form

$$\frac{\partial}{\partial t} y_r = -K_r y_r + S_r. \tag{1}$$

Each component of Eq. (1) is a function of x, a dimensionless measure of the velocity of a Na atom along the direction of a monochromatic laser pumping beam and time t, which we measure in units of the "velocity damping" time. The element of the atomic density matrix for atoms with velocities between

x and $x + dx$ is $y_r\,dx = y_r(x,t)dx$. The subscript r denotes the velocity-independent relaxation rate r. The real part of r is proportional to the rate of spin-changing collisions and the imaginary part of r is proportional to the Larmor precession rate—or to some other Bohr frequency of the atom. Different elements y_r of the density matrix will have different relaxation rates r. The source rate $S_r = S_r(x,t)$ is proportional to the optical pumping rate and it is a linear combination of all of the y_r of the system.

The collisional damping operator K_r can be represented in various ways, notably as the kernel of an integral transform

$$K_r y_r(x,t) = \int_{-\infty}^{\infty} dx'(x|K_r|x')y_r(x',t). \tag{2}$$

The velocity of an optically pumped alkali-metal atom will change by a small or large fraction of its mean thermal velocity depending on whether the collision is "weak" or "strong." The kernel K_r will be more "diagonal" in velocity space for weak collisions than for strong collisions. A comprehensive review of the "linear transport equation" or "Boltzmann transport equation" (1) was given by Berman [8]. With minor changes in notation, the kernel K_r of Eq. (1) is often written as $(x|K_r|x') = (r+1)\delta(x-x') - (x|W|x')$ and $(x|W|x')$ is called the collision kernel [7,9].

The formal solution to Eq. (1) is

$$y_r(x,t) = \int_0^{\infty} d\tau \int_{-\infty}^{\infty} dx'(x|T_r(\tau)|x')S_r(x',t-\tau), \tag{3}$$

where a formal expression for the impulse-response function is

$$T_r(\tau) = e^{-K_r\tau}. \tag{4}$$

For a time-independent source term $S_r = S_r(x)$, the transients associated with Eq. (1) die down and the time-independent, steady-state density matrix $y_r(x)$ is given by $K_r y_r = S_r$, the solution of which can be written as

$$y_r(x) = \int_{-\infty}^{\infty} dx'(x|G_r|x')S_r(x'). \tag{5}$$

A formal expression for the Green's function is

$$G_r = \frac{1}{K_r} = \int_0^{\infty} T_r(\tau)d\tau. \tag{6}$$

As we will show in this article, the fundamental operators K_r, $T_r(\tau)$, and G_r have various representations, some more convenient for numerical computation and some more convenient for abstract discussions. For example, G_r can be expressed as an infinite series (253) of Hermite polynomials, or alternately, as an infinite series (254) of Gaussians. For the limiting cases of weak or strong collisions the fundamental operators also have nonseries expressions: Eqs. (84), (86), and (132) or Eqs. (261) through (263).

As an example of the different behavior of velocity distributions that evolve because of weak or strong collisions, consider a Gaussian initial distribution $y_0(x,0) \propto \exp -(x-x_0)^2/2\sigma_0^2$ that is created by an impulsive source $S(x,t) = y_0(x,0)\delta(t-\Delta t)$, where $\Delta t \to 0$ is a small, positive time increment. We see from Eq. (3) that the distribution at time t will be

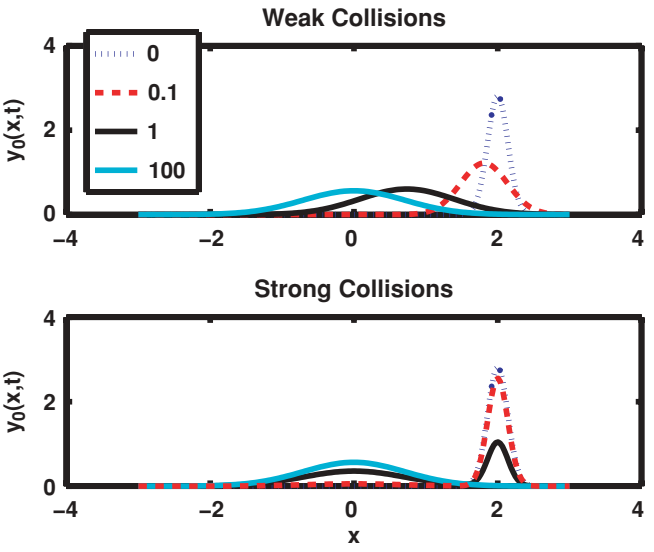

FIG. 1. (Color online) Source-free time evolution from Eq. (7) of an initial, Gaussian velocity distribution $y_0(x,0) = e^{(x-\bar{x}_0)^2/2\sigma_0^2}/\sqrt{2\pi\sigma_0^2}$ with $\sigma_0^2 = 1/50$ and $\bar{x}_0 = 2$ for weak and strong collisions and with $r = 0$. The curves are plotted for $t = 0, 0.1, 1,$ and 100. In this and subsequent figures, all quantities plotted are dimensionless.

$$y_0(x,t) = \int_{-\infty}^{\infty} (x|T_0(t)|x')y_0(x',0)dx'. \tag{7}$$

For simplicity, we let $r = 0$. In Fig. 1 we show the free evolution, evaluated with Eq. (7), of the same initial Gaussian distribution of velocities for the limits of weak and strong collisions, with impulse response functions $T_0(t)$ given by Eqs. (86) and (262), respectively. Salient features that one can see in Fig. 1 are:

1. For the weak-collision limit, the initial Gaussian distribution continuously changes its variance σ_t^2 and its mean $\bar{x}_t$, but remains a Gaussian until it settles down to a Maxwellian distribution, that is, a Gaussian distribution with mean $\bar{x}_0 = 0$ and variance $\sigma_\infty^2 = 1/2$. One can use Eq. (86) to show that if the initial distribution has a variance σ_0^2 and mean $\bar{x}_0$ at time $t = 0$, then $\sigma_t^2 = (\sigma_0^2 - 1/2)e^{-2t} + 1/2$ and $\bar{x}_t = \bar{x}_0 e^{-t}$. Non-Gaussian initial distributions also evolve to the Maxwellian distribution, but they change their shapes in the process.

2. For the strong-collision limit, the initial Gaussian distribution damps exponentially, with no change in its initial variance σ_0^2 or mean $\bar{x}_0$. This represents atoms that have not yet had collisions. Atoms that have had collisions immediately assume a Maxwellian distribution with a variance $\sigma_\infty = 1/2$ and with a mean $\bar{x}_\infty = 0$. The distribution becomes bimodal at intermediate times. The part of the distribution representing atoms that have not yet had a strong collision undergoes simple exponential damping for any shape of the initial velocity distribution.

3. Both weak and strong collisions lead to the same Maxwellian distribution at late times, with variance $\sigma_\infty^2 = 1/2$. So any experimental phenomenon that depends mostly on final-state distributions will not be sensitive to whether

the collisions are weak or strong. Steady-state experiments to investigate the relative importance of weak and strong velocity-changing collisions must be designed with velocity-independent damping rates r that are large enough to maximize the contributions of intermediate times, when there is the largest possible difference between the evolving distributions for weak and strong collisions.

We devoted about half of this article to the optical-pumping physics that motivated us and to simple examples of how to solve problems with the formalism we introduce. The remainder of the article is devoted to details of the mathematics, which includes a brief review of previous work on similar problems as well as new methods that we hope will be useful well beyond the optical-pumping physics of guidestars.

II. EVOLUTION

We consider a hypothetical Na isotope with nuclear spin quantum number $I = 0$. The procedures we outline below work just as well for a real ^{23}Na atom with $I = 3/2$, but because of the much larger size of the density matrix, 8×8 instead of 2×2, illustrating the discussions of this article with a real ^{23}Na atom will complicate the discussion without adding additional insight into the physics. The ground-state Hamiltonian for the hypothetical atom is

$$H = \hbar\omega S_z, \quad \text{where} \quad \omega = \frac{g_S \mu_B B}{\hbar}. \tag{8}$$

Here $g_S = 2.00231$ is the g value of the electron, $\mu_B = 9.2741 \times 10^{-21}$ erg gauss^{-1} is the Bohr magneton, and $2\pi\hbar = h = 6.6262 \times 10^{-27}$ erg s is Planck's constant. The hypothetical atom has two energy sublevels with azimuthal quantum numbers $\mu = \alpha = 1/2$ or $\mu = \beta = -1/2$

$$S_z|\alpha\rangle = \alpha|\alpha\rangle = \tfrac{1}{2}|\alpha\rangle, \quad \text{and} \quad S_z|\beta\rangle = \beta|\beta\rangle = -\tfrac{1}{2}|\beta\rangle. \tag{9}$$

We describe the optically pumped Na atoms with a velocity-dependent density matrix

$$\phi = \sum_{\mu\nu} |\mu\rangle\phi_{\mu\nu}\langle\nu|. \tag{10}$$

The density matrix $\phi = \phi(v, t)$ of Eq. (10) depends on time t and on the velocity v of the atom along the direction of the light beam. We assume that the components of the velocity transverse to the laser beam have a Maxwellian distribution at the local atmospheric temperature T. The density matrix of the atoms with velocities between v and $v + dv$ is $d\rho = \phi dv$.

If we integrate over all velocity groups, we get the familiar spin density matrix

$$\rho = \int_{-\infty}^{\infty} \phi dv. \tag{11}$$

For the hypothetical atom, we can group the elements of the density matrix $\phi_{\mu\nu}$ as a 2×2 matrix ϕ in Schrödinger space

$$\phi = \begin{bmatrix} \phi_{\alpha\alpha} & \phi_{\alpha\beta} \\ \phi_{\beta\alpha} & \phi_{\beta\beta} \end{bmatrix} = \sum_{\mu\nu} |\mu\rangle\langle\nu|\phi_{\mu\nu}, \tag{12}$$

or as a 4×1 column vector $|\phi)$ in Liouville space

$$|\phi) = \begin{bmatrix} \phi_{\alpha\alpha} \\ \phi_{\beta\alpha} \\ \phi_{\alpha\beta} \\ \phi_{\beta\beta} \end{bmatrix} = \sum_k |k)(k|\phi). \tag{13}$$

The column vector $|\phi)$ of Eq. (13) is formed from the matrix ϕ of Eq. (12) by placing each column of ϕ below the one to its left. The Schrödinger-space basis operators $|\mu\rangle\langle\nu|$ are in one-to-one correspondence with the Liouville-space basis vectors $|k)$, with $(k|\phi) = \mathrm{Tr}[(|\mu\rangle\langle\nu|)^\dagger\phi] = \phi_{\mu\nu}$. For our simple, hypothetical atom there is little reason to use the Liouville-space representation of Eq. (13) in preference to the conventional representation of Eq. (12). For real ^{23}Na atoms, with many more sublevels, some of the substantial advantages of Liouville space are:

1. The equations describing spin relaxation look simpler for Liouville space.

2. Both isentropic processes, like the evolution of atoms under the influence of a common Hamiltonian and processes like spin relaxation or optical pumping that increase or decrease the spin entropy are described by analogous superoperators in Liouville space.

3. It is easier to write and debug computer code based on the Liouville-space formalism, since the coding statements look very similar to theoretical equations in the text.

We will therefore continue our discussion using the Liouville-space formalism, the first example of which is Eq. (13).

Following traditional Dirac notation, we use a ket, for example $|\alpha\rangle$, to denote a column vector in Schroedinger space, and we use a bra, for example $\langle\alpha|$, to denote the Hermitian conjugate of the ket—a row vector. In like manner we use right parenthesis, for example $|\phi)$, to denote a column vector in Liouville space, and we use a left parenthesis, for example $(\phi|$, to denote the Hermitian conjugate of the column vector—a row vector. Later we will encounter non-orthonormal basis vectors $|\gamma_k)$ for Liouville space, analogous to the non-orthnormal basis vectors for crystal lattices. We denote the "reciprocal basis vectors," with a double left parenthesis, for example $(\!(\gamma_k|$. When we use the double-parenthesis notation, it is implied that $(\!(\gamma_k|$ is not the same as $(\gamma_k|$. The two row vectors may point in different directions. Further discussion of these and related issues can be found in the book, *Optically Pumped Atoms*, by Happer, Jau, and Walker [10]

a. Evolution due to the Hamiltonian. The Hamiltonian will cause the density matrix ϕ to evolve at the rate

$$\frac{\partial}{\partial t}\phi = \frac{1}{i\hbar}[H, \phi]. \tag{14}$$

The Liouville-space version of Eq. (14) is

$$\frac{\partial}{\partial t}|\phi) = \frac{1}{i\hbar} H^{\copyright}|\phi). \tag{15}$$

The "commutator superoperator" is the difference of Kronecker products,

$$H^{\copyright} = 1^{\{g\}} \otimes H - H^T \otimes 1^{\{g\}}. \tag{16}$$

Here H^T is the transpose of H and the unit operator for ground-state atoms is

$$1^{\{g\}} = \sum_{\mu} |\mu\rangle\langle\mu|. \tag{17}$$

There is a clear introduction to superoperators in *Principles of Magnetic Resonance in One and Two Dimensions* by Ernst, Bodenhausen, and Wokaun [11]. Unlike our convention, where we construct the column vector $|\phi)$ from the columns of ϕ, Ernst *et al.* constructed $|\phi)$ from the rows of ϕ. This causes some minor changes in the definitions of the superoperators. For the hypothetical atom and its simple Hamiltonian (8) we have

$$H^{\textcircled{c}} = \hbar\omega \begin{bmatrix} 0 & 0 & 0 & 0 \\ 0 & -1 & 0 & 0 \\ 0 & 0 & 1 & 0 \\ 0 & 0 & 0 & 0 \end{bmatrix}. \tag{18}$$

b. Evolution due to spin relaxation. We assume that the longitudinal and transverse spin-relaxation rates are equal and given by the S-damping rate $\Gamma_{\rm sd}$. Then S-damping collisions cause the amplitudes $\phi_{\mu\nu}$ to change at the rate

$$\begin{aligned} \dot{\phi}_{\alpha\alpha} &= \tfrac{1}{2}\Gamma_{\rm sd}(\phi_{\beta\beta} - \phi_{\alpha\alpha}), \\ \dot{\phi}_{\beta\alpha} &= -\Gamma_{\rm sd}\phi_{\beta\alpha}, \\ \dot{\phi}_{\alpha\beta} &= -\Gamma_{\rm sd}\phi_{\alpha\beta}, \\ \dot{\phi}_{\beta\beta} &= \tfrac{1}{2}\Gamma_{\rm sd}(\phi_{\alpha\alpha} - \phi_{\beta\beta}). \end{aligned} \tag{19}$$

This can be written as the matrix equation

$$\frac{\partial}{\partial t}|\phi) = -\Gamma_{\rm sd} A_{\rm sd}|\phi). \tag{20}$$

The dimensionless, S-damping matrix is

$$A_{\rm sd} = \frac{1}{2}\begin{bmatrix} 1 & 0 & 0 & -1 \\ 0 & 2 & 0 & 0 \\ 0 & 0 & 2 & 0 \\ -1 & 0 & 0 & 1 \end{bmatrix}. \tag{21}$$

The S-damping rate is

$$\Gamma_{\rm sd} = [N]\bar{v}\sigma_{\rm sd}, \tag{22}$$

$\bar{v}$ is the mean relative velocity between an Na atom and an atmospheric constituent—like an N_2 or O_2 molecule or an O atom—of total number density $[N]$. The mean spin-relaxation cross section is $\sigma_{\rm sd}$. The rate coefficients $\bar{v}\sigma_{\rm sd}$ for collisions of Na atoms with O_2 molecules or O atoms, both with unpaired spins, will be on the order of $\bar{v}\sigma_{\rm sd} \approx 10^{-9}$ cm^3 s^{-1}, similar to the rate coefficients for spin-exchange collisions between pairs of alkali-metal atoms [12]. For diamagnetic species like N_2 or Ar, the rate coefficients will be many orders of magnitude smaller [12], typically $\bar{v}\sigma_{\rm sd} \approx 10^{-18}$ cm^3 s^{-1}. So the mean rate coefficient will be determined by the fraction of the atmospheric particles that are O_2 molecules or O atoms. This fraction will depend on altitude and on upper atmospheric "weather," but a representative fraction will be about 0.3, so a representative S-damping rate (22) will be $\Gamma_{\rm sd} = 3 \times 10^4$ s^{-1}.

c. Evolution due to velocity-changing collisions. As mentioned in connection with Eq. (1), we assume that the evolution of the density matrix due to velocity-changing collisions can be written as

$$\frac{\partial}{\partial t}\phi(v) = -\int (v|K|v')\phi(v')dv'. \tag{23}$$

We make the simplifying assumption that the collisional change in spin is uncorrelated with the collisional change in velocity. There are theoretical reasons to question this independence [8] and experimental tests are needed to see how well this simplifying assumption works for Na atoms under guidestar conditions.

Let $\chi(v)dv$ be the probability to find atoms with velocities between v and $v + dv$ where

$$\chi(v) = \mathrm{Tr}[\phi(v)]. \tag{24}$$

The mean velocity of the atoms along the laser beam is then

$$\langle v\rangle = \int v\chi(v)dv. \tag{25}$$

For the models we consider in this article, velocity-changing collisions will cause $\langle v\rangle$ to decay exponentially at the "velocity-damping rate"

$$\Gamma_{\rm vd} = -\frac{d}{dt}\ln\langle v\rangle = \frac{1}{\langle v\rangle}\int v(v|K|v')\chi(v')dv'. \tag{26}$$

d. Weak velocity-changing collisions. We begin by discussing weak, velocity-changing collisions, where the velocity increments per collisions are so small that it makes sense to use the concept of diffusion in velocity space. We will defer our discussion of strong collisions until we explain the basic physics associated with weak collisions. The sum of the diffusion current density $-D_v\partial|\phi)/\partial v$ and the drift current density $-\Gamma_{\rm vd}v|\phi)$ gives the total current density

$$j|\phi), \quad \text{with} \quad j = -D_v\frac{\partial}{\partial v} - \Gamma_{\rm vd}v. \tag{27}$$

The diffusion coefficient in velocity space is D_v. The viscous damping rate of the velocity will be

$$\Gamma_{\rm vd} = [N]\bar{v}\sigma_{\rm vd}. \tag{28}$$

If l is the mean free path of an Na atom, we know that we should have $\Gamma_{\rm vd} \approx \bar{v}/l$. Estimating l from measured diffusion coefficients of Na atoms in N gas [12] we find that a representative rate coefficient for velocity damping is $\bar{v}\sigma_{\rm vd} = 10^{-10}$ cm^3 s^{-1}, about a factor of 3 smaller than the rate coefficient $\Gamma_{\rm sd}$ of Eq. (22) for S-damping. The exact values of $\Gamma_{\rm vd}$ and $\Gamma_{\rm sd}$ are not important, but the fact that they are of the same order of magnitude is unusual, since in conventional gas cells, where the buffer gas contains no paramagnetic species like O_2 molecules or O atoms, $\Gamma_{\rm sd}$ is many orders of magnitude smaller than $\Gamma_{\rm vd}$.

Substituting Eq. (27) into the equation of continuity

$$\frac{\partial}{\partial t}|\phi) + \frac{\partial}{\partial v}j|\phi) = 0, \tag{29}$$

we find the evolution equation for weak collisions

$$\frac{\partial}{\partial t}|\phi) = D_v\frac{\partial^2}{\partial v^2}|\phi) + \Gamma_{\rm vd}\frac{\partial}{\partial v}v|\phi). \tag{30}$$

From Eqs. (30) and (2) we see that the kernel for weak collisions is

$$(v|K|v') = -\left(D_v \frac{\partial^2}{\partial v^2} + \Gamma_{\rm vd} \frac{\partial}{\partial v} v\right) \delta(v - v'). \quad (31)$$

In steady state $\partial|\phi)/\partial t = 0$ and Eq. (30) implies that the velocity dependence of $|\phi)$ is

$$\frac{\partial}{\partial v} j|\phi) = 0, \quad \text{or} \quad j|\phi) = \text{constant}. \quad (32)$$

There can be no current of atoms with infinite velocity, so the constant, steady-state current of Eq. (32) must be $j|\phi) = 0$. Then we can integrate Eq. (32), with j given by Eq. (27), to find a normalized distribution

$$|\phi_1) = |\rho_1) \frac{e^{-v^2/2\sigma_v^2}}{\sqrt{2\pi\sigma_v^2}}, \quad \text{where} \quad \sigma_v^2 = \frac{D_v}{\Gamma_{\rm vd}}. \quad (33)$$

In view of Boltzmann statistics, we must also have $\sigma_v^2 = k_B T/M$, where M is the mass of the atom, k_B is Boltzmann's constant, and T is the absolute temperature. For ^{23}Na guidestar atoms, with a representative temperature $T = 180$ K, the standard deviation is

$$\sigma_v = 2.55 \times 10^4 \text{ cm s}^{-1}. \quad (34)$$

Equating the velocity variance of Eq. (33) to that demanded by Boltzmann statistics we find the Einstein-Smoluchowski relation [13]

$$M D_v = \Gamma_{\rm vd} k_B T. \quad (35)$$

e. Optical pumping. For simplicity we suppose that the hypothetical atom is pumped by D_1 light to the $^2P_{1/2}$ state. The key parts of the discussion in the following do not change if we consider D_2 pumping to the $^2P_{3/2}$ state or pumping of a real Na atom. Let the spectrally resolved energy flux of the light with optical frequencies between $\nu = \omega/(2\pi)$ and $\nu + d\nu$ be $F(\nu)d\nu$ (typical units of F are mW cm^{-2} MHz^{-1}). Integrating over all optical frequencies ν, we find the total energy flux I (typical units of I are mW cm^{-2}), and the mean frequency ν_0 are

$$I = \int F(\nu)d\nu, \quad \text{and} \quad \nu_0 = \frac{1}{I}\int F(\nu)\nu d\nu. \quad (36)$$

The mean optical pumping rate of unpolarized atoms with velocity v along the light beam is

$$\Gamma_{\rm op}(v) = \frac{1}{\hbar\omega_{\rm op}} \int_0^\infty \sigma_{\rm op}(v, \nu) F(\nu) d\nu. \quad (37)$$

The absorption cross section is

$$\sigma_{\rm op}(v, \nu) = \frac{2\pi r_e c f \gamma_2}{\gamma_2^2 + (\omega - \omega_{\rm op}[1 + v/c])^2}. \quad (38)$$

Here $\omega_{\rm op} = 2\pi c/\lambda_{\rm op}$ is the resonance optical absorption frequency for pumping atoms at rest into the excited state. The corresponding wavelength is $\lambda_{\rm op} = 589.8$ nm. The speed of light is $c = 3 \times 10^{10}$ cm s^{-1}, the classical electron radius is $r_e = 2.82 \times 10^{-13}$ cm, and $f = 0.322$ is the oscillator strength. The homogeneous "$1/T_2$" linewidth of the optical absorption line is

$$\gamma_2 = \frac{1}{2\tau} + \gamma_c, \quad (39)$$

where $\tau = 16.23$ ns is the spontaneous radiative lifetime of the excited state and $\gamma_c = \bar{v}\sigma_c[N]$ is the collisional broadening of the optical line. For a representative optical line-broadening coefficient $\bar{v}\sigma_c = 2 \times 10^{-9}$ cm^{3}s^{-1} and a number density $[N] = 10^{14}$ cm^{-3}, we will have $\gamma_c = 2 \times 10^5$ s^{-1}, compared to $1/(2\tau) = 3.1 \times 10^7$ s^{-1}. So the homogeneous optical absorption linewidth of Na guidestar atoms is almost completely due to the natural spontaneous lifetime of the atoms, with a contribution from collisions of only about 1%. We note the area identities for the cross section

$$\int \sigma_{\rm op}(v, \nu)d\nu = \pi r_e c f, \quad \text{and} \quad \int \sigma_{\rm op}(v, \nu)d\nu = \pi r_e c f \lambda_{\rm op}. \quad (40)$$

We define a resonant velocity by

$$v_0 = \frac{\int \Gamma_{\rm op} v dv}{\int \Gamma_{\rm op} dv}. \quad (41)$$

The resonant velocity v_0 can be used to define a dimensionless lineshape function $g = g(v)$

$$g = \frac{\Gamma_{\rm op}(v)}{\Gamma_{\rm op}(v_0)}, \quad \text{with} \quad g(v_0) = 1. \quad (42)$$

We define a velocity width Δv

$$\Delta v = \int g dv. \quad (43)$$

It will be useful to define a saturation flux I_s, at which the optical pumping rate $\Gamma_{\rm op}(v_0)$ is equal to the spontaneous decay rate $1/\tau$ of an excited atom

$$I_{\rm s} = \frac{I}{\Gamma_{\rm op}(v_0)\tau}. \quad (44)$$

f. Gaussian spectral profiles. For modeling it will be convenient to take a Gaussian spectral profile for the pumping light

$$F(\nu) = \frac{I e^{-\frac{(\nu-\nu_0)^2}{2\sigma_\nu^2}}}{\sqrt{2\pi\sigma_\nu^2}}. \quad (45)$$

The peak frequency is $\nu_0 = \omega_0/2\pi$ and the variance is σ_ν^2. Substituting Eq. (45) into Eq. (37) we find that the lineshape function (42) becomes

$$g = \text{Re}\left(\frac{Z(z)}{Z(z_o)}\right) = \text{Re}\left(\frac{w(z)}{w(z_o)}\right). \quad (46)$$

Here Z is the plasma dispersion function and w is the closely related Faddeeva function [14], both discussed in more detail in Sec. IV D. Both have the same complex arguments

$$z = \frac{1}{2\pi\sigma_v\sqrt{2}}(\omega_{\rm op}[1 + v/c] - \omega_o + i\gamma_2), \quad \text{and} \quad z_o = \frac{i\gamma_2}{2\pi\sigma_v\sqrt{2}}. \quad (47)$$

The resonant velocity of Eq. (41) becomes

$$v_o = c(\omega_o/\omega_{\rm op} - 1). \quad (48)$$

The velocity width (43) and the saturation flux (44) become

$$\Delta v = \frac{\lambda_{\rm op}\sigma_v\sqrt{2\pi}}{w(z_o)}, \quad \text{and} \quad I_{\rm s} = \frac{4\hbar\gamma_2\Delta v}{r_e\lambda_{\rm op}^2 f}. \tag{49}$$

In the monochromatic limit when $\sigma_v \to 0$ and $|z_o| \gg 1$, we can use the asymptotic expression (200) of the Faddeeva function to show that

$$\Delta v \to \frac{\lambda_{\rm op}\gamma_2}{2}, \quad \text{and} \quad I_{\rm s} \to \frac{2\hbar\gamma_2^2}{r_e\lambda_{\rm op} f}, \quad \text{for} \quad \sigma_v \ll \gamma_2. \tag{50}$$

The monochromatic limit (50) gives the minimum saturation flux, which has the value

$$I_{\rm s} = 38 \text{ mW cm}^{-2}, \tag{51}$$

for the D_1 line of Na and negligible collisional broadening. For nonzero spectral widths, the saturation flux is larger. When the spectral width σ_v is large enough that $|z_o| \ll 1$, we can use Eq. (198) with Eq. (49) to show that

$$\Delta v \to \lambda_{\rm op}\sigma_v\sqrt{2\pi}, \quad \text{and} \quad I_{\rm s} \to \frac{\hbar\sigma_v\gamma_2\sqrt{32\pi}}{r_e\lambda_{\rm op} f}, \quad \text{for} \quad \sigma_v \gg \gamma_2. \tag{52}$$

In subsequent discussions, we will assume laser intensities $I \ll I_{\rm s}$, so that we can neglect the effects of saturation and stimulated emission by excited atoms. Accounting for saturation does not lead to any qualitative changes in our discussion of the combined effects of velocity-changing collisions and depolarization processes.

g. Spin evolution due to optical pumping. For pumping to the $^2P_{1/2}$ state, the light can only pump out of the spin-down ground-state sublevel $|\beta\rangle$ of the hypothetical atom. The amplitudes $\phi_{\mu\nu}$ will change at the rate

$$\begin{aligned} \dot\phi_{\alpha\alpha} &= \tfrac{2}{3}\Gamma_{\rm op}\phi_{\beta\beta}, \\ \dot\phi_{\beta\alpha} &= -\Gamma_{\rm op}\phi_{\beta\alpha}, \\ \dot\phi_{\alpha\beta} &= -\Gamma_{\rm op}\phi_{\alpha\beta}, \\ \dot\phi_{\beta\beta} &= -2\Gamma_{\rm op}\phi_{\beta\beta} + \tfrac{4}{3}\Gamma_{\rm op}\phi_{\beta\beta}. \end{aligned} \tag{53}$$

The terms on the right of Eq. (53) with negative signs describe depopulation pumping at a mean rate $\Gamma_{\rm op} = \Gamma_{\rm op}(v)$, which will depend on how close the velocity v is to the resonant velocity $c(\omega/\omega_{\rm op} - 1)$, picked out by the light of frequency ω. The terms on the right of Eq. (53) with positive signs describe repopulation pumping, with 2/3 of the atoms pumped out of the spin-down sublevel $|\beta\rangle$, returned by spontaneous decay, and the other 1/3 transferred to the spin-up sublevel $|\alpha\rangle$. Depopulation pumping destroys the coherences $\rho_{\beta\alpha}$ and $\rho_{\alpha\beta}$ at the mean pumping rate and no coherence is returned by repopulation pumping. Note that we can write Eq. (53) as a special case of the matrix equation

$$\frac{\partial}{\partial t}|\phi) = -\Gamma_{\rm op}A_{\rm op}(\mathbf{n})|\phi), \tag{54}$$

which describes pumping of the atoms into the $^2P_{1/2}$ excited state by light that is right-circularly polarized along the direction of propagation $\mathbf{n}$. Comparing Eq. (53) with Eq. (54) we see that the dimensionless pumping matrix is

$$A_{\rm op}(\mathbf{z}) = \frac{1}{3}\begin{bmatrix} 0 & 0 & 0 & -2 \\ 0 & 3 & 0 & 0 \\ 0 & 0 & 3 & 0 \\ 0 & 0 & 0 & 2 \end{bmatrix}. \tag{55}$$

For guidestars the pumping light is seldom parallel to the geomagnetic field, which we have taken to define the z axis of our coordinate system. We need an expression analogous to Eq. (55) for an arbitrary direction of propagation. To find such an expression, we generate row and column vectors for Liouville space from the unit operator and the Pauli spin matrices of Schrödinger space

$$\begin{aligned} 1^{\{g\}} &= \begin{bmatrix} 1 & 0 \\ 0 & 1 \end{bmatrix}, \quad |1^{\{g\}}) = \begin{bmatrix} 1 \\ 0 \\ 0 \\ 1 \end{bmatrix}, \\ (1^{\{g\}}| &= [1 \quad 0 \quad 0 \quad 1], \end{aligned} \tag{56}$$

$$\begin{aligned} S_x &= \frac{1}{2}\begin{bmatrix} 0 & 1 \\ 1 & 0 \end{bmatrix}, \quad |S_x) = \frac{1}{2}\begin{bmatrix} 0 \\ 1 \\ 1 \\ 0 \end{bmatrix}, \\ (S_x| &= \frac{1}{2}[0 \quad 1 \quad 1 \quad 0], \end{aligned} \tag{57}$$

$$\begin{aligned} S_y &= \frac{1}{2i}\begin{bmatrix} 0 & 1 \\ -1 & 0 \end{bmatrix}, \quad |S_y) = \frac{1}{2i}\begin{bmatrix} 0 \\ -1 \\ 1 \\ 0 \end{bmatrix}, \\ (S_y| &= -\frac{1}{2i}[0 \quad -1 \quad 1 \quad 0], \end{aligned} \tag{58}$$

$$\begin{aligned} S_z &= \frac{1}{2}\begin{bmatrix} 1 & 0 \\ 0 & -1 \end{bmatrix}, \quad |S_z) = \frac{1}{2}\begin{bmatrix} 1 \\ 0 \\ 0 \\ -1 \end{bmatrix}, \\ (S_z| &= \frac{1}{2}[1 \quad 0 \quad 0 \quad -1]. \end{aligned} \tag{59}$$

Using Eqs. (56) through (59), we can write Eq. (55) as

$$A_{\rm op}(\mathbf{z}) = \tfrac{2}{3}\{3|\mathbf{S}) \cdot (\mathbf{S}| - |S_z)(S_z| - |S_z)(1^{\{g\}}|\}. \tag{60}$$

We note that

$$|\mathbf{S}) \cdot (\mathbf{S}| = |S_x)(S_x| + |S_y)(S_y| + |S_z)(S_z| = \tfrac{1}{2}A_{\rm sd}, \tag{61}$$

with the S-damping matrix given by Eq. (21). It is clear that if the light is propagating along the unit vector $\mathbf{n}$ instead of along the unit vector $\mathbf{z}$ that Eq. (60) becomes

$$A_{\rm op}(\mathbf{n}) = \tfrac{2}{3}\{3|\mathbf{S}) \cdot (\mathbf{S}| - |\mathbf{n}\cdot\mathbf{S})(\mathbf{n}\cdot\mathbf{S}| - |\mathbf{n}\cdot\mathbf{S})(1^{\{g\}}|\}. \tag{62}$$

For example, if the light is propagating along the x axis (perpendicular to the direction of the magnetic field) so $\mathbf{n} = \mathbf{x}$,

we find

$$A_{\rm op}(\mathbf{x}) = \frac{1}{6}\begin{bmatrix} 3 & 0 & 0 & -3 \\ -2 & 5 & -1 & -2 \\ -2 & -1 & 5 & -2 \\ -3 & 0 & 0 & 3 \end{bmatrix}. \tag{63}$$

h. Absorption per atom. From inspection of Eq. (53) we see that the absorption rate (depopulation pumping rate) of atoms with velocities between v and $v + dv$ is

$$2\Gamma_{\rm op}\phi_{\beta\beta}dv = (\Gamma_{\rm dp}|\phi)dv. \tag{64}$$

The total absorption rate from polarized atoms of all velocities is

$$\langle\delta\Gamma\rangle = \int (\Gamma_{\rm dp}|\phi)dv. \tag{65}$$

As shown in Eq. (64), only atoms in the spin-down sublevel $|\beta\rangle$ can absorb right-circularly polarized light propagating along the z axis. Generalizing Eq. (64) with arguments similar to those previously, we see that the absorption per polarized atom of light propagating along the unit vector $\mathbf{n}$ can be represented by the row vector

$$(\Gamma_{\rm dp}| = \Gamma_{\rm op}\{(1^{\{g\}}| - 2(\mathbf{n}\cdot\mathbf{S}|\}. \tag{66}$$

In experiments, one often observes the change, ΔI, in the intensity of the pumping light. Since each absorbed photon removes an energy quantum, $\hbar\omega_{\rm op}$, from the pumping beam, the intensity change is

$$\Delta I = -\hbar\omega_{\rm op}[{\rm Na}]\int\langle\delta\Gamma\rangle dV. \tag{67}$$

Here the integral extends over the volume elements, dV, of the illuminated vapor and [Na] is the number density of Na atoms.

i. Relaxation modes. Adding the evolution due to the Hamiltonian (15), spin-changing collisions (20), velocity-changing collisions (30), and optical pumping (54), we find that the net evolution of the density matrix in the limit of weak velocity changing collisions

$$\frac{\partial}{\partial t}|\phi) = D_v\frac{\partial^2}{\partial v^2}|\phi) + \Gamma_{\rm vd}\frac{\partial}{\partial v}v|\phi) - \Gamma|\phi) - \Gamma_{\rm op}A_{\rm op}|\phi). \tag{68}$$

The evolution due to the Hamiltonian and collisional spin relaxation is described by the operator

$$\Gamma = \Gamma_{\rm sd}A_{\rm sd} + \frac{i}{\hbar}H^{\copyright} = \Gamma = \sum_{j=1}^{m}\gamma_j|\gamma_j)(\!(\gamma_j|. \tag{69}$$

The damping matrix Γ has eigenvalues γ_j and right and left eigenvectors, $|\gamma_j)$, and $(\!(\gamma_j|$, defined by

$$\Gamma|\gamma_j) = \gamma_j|\gamma_j), \quad \text{and} \quad (\!(\gamma_j|\Gamma = (\!(\gamma_j|\gamma_j. \tag{70}$$

We assume that the eigenvectors are linearly independent and that we can normalize them such that

$$(\!(\gamma_j|\gamma_k) = \delta_{jk} \quad \text{and} \quad \sum_{j=1}^{m}|\gamma_j)(\!(\gamma_j| = 1, \tag{71}$$

where $m = 4(2I+1)^2$ is the number of polarization modes of an alkali-metal atom with nuclear spin quantum number I.

We can use Eqs. (21) and (18) to write Eq. (69) as

$$\Gamma = \frac{\Gamma_{\rm sd}}{2}\begin{bmatrix} 1 & 0 & 0 & -1 \\ 0 & 2 & 0 & 0 \\ 0 & 0 & 2 & 0 \\ -1 & 0 & 0 & 1 \end{bmatrix} + i\omega\begin{bmatrix} 0 & 0 & 0 & 0 \\ 0 & -1 & 0 & 0 \\ 0 & 0 & 1 & 0 \\ 0 & 0 & 0 & 0 \end{bmatrix}. \tag{72}$$

Using Eqs. (70) through (72) we write the eigenvalues and eigenvectors of Eq. (72) as

$$\gamma_1 = 0, \quad |\gamma_1) = \tfrac{1}{2}|1^{\{g\}}), \quad (\!(\gamma_1| = (1^{\{g\}}|, \tag{73}$$

$$\gamma_2 = \Gamma_{\rm sd}, \quad |\gamma_2) = |S_z), \quad (\!(\gamma_2| = 2(S_z|. \tag{74}$$

The column vectors $|1^{\{g\}})$ and $|S_z)$ were given by Eqs. (56) and (59). The remaining eigenvalues and eigenvectors are

$$\gamma_3 = \Gamma_{\rm sd} - i\omega, \quad |\gamma_3) = |S_-) = \begin{bmatrix} 0 \\ 1 \\ 0 \\ 0 \end{bmatrix}, \quad (\!(\gamma_3| = (S_-| = [0 \quad 1 \quad 0 \quad 0], \tag{75}$$

and

$$\gamma_4 = \Gamma_{\rm sd} + i\omega, \quad |\gamma_4) = |S_+) = \begin{bmatrix} 0 \\ 0 \\ 1 \\ 0 \end{bmatrix}, \quad (\!(\gamma_4| = (S_+| = [0 \quad 0 \quad 1 \quad 0]. \tag{76}$$

The raising and lowering operators for the electron spin are $S_\pm = S_x \pm iS_y$, so Eqs. (75) and (76) follow from Eqs. (57) and (58).

For real atoms with nonzero nuclear spins and more complicated spin relaxation mechanisms, the slowest mode will still have $\gamma_1 = 0$ and eigenvectors $|\gamma_1)$ and $(\!(\gamma_1|$ analogous to those of Eq. (73)—provided that the collisions do not destroy atoms—for example, by irreversible chemical reactions.

j. Dimensionless quantities. For further analysis it will be convenient to introduce dimensionless versions of the quantities in Eq. (68). We measure time in units of the mean time between velocity-changing collisions

$$\theta = \Gamma_{\rm vd}t. \tag{77}$$

Where no confusion is likely we will denote the dimensionless time θ with the same symbol t as the time in seconds. We measure velocity in units of a characteristic velocity v_D

$$x = \frac{v}{v_D}. \tag{78}$$

It is convenient to let the characteristic velocity be $\sqrt{2}$ times larger than the standard deviation of Eq. (33)

$$v_D = \sigma_v\sqrt{2}, \quad \text{or} \quad v_D = 3.61\times10^4\ {\rm cm\ s^{-1}}. \tag{79}$$

The dimensionless version of the density matrix is

$$|\Phi) = v_D|\phi), \quad \text{with projections} \quad \Phi_k = (\!(\gamma_k|\Phi). \tag{80}$$

The dimensionless version of the current operator j of Eq. (27) for weak collisions is

$$J = \frac{j}{\Gamma_{\rm vd} v_D} = -\frac{1}{2}\frac{\partial}{\partial x} - x, \quad \text{with projections} \quad J_k = (\!(\gamma_k|J|\Phi)\!). \tag{81}$$

The characteristic optical pumping rate p is

$$p = \frac{\Gamma_{\rm op}(v_0)}{\Gamma_{\rm vd}} = \frac{I}{I_p}, \quad \text{where} \quad I_p = I_s \Gamma_{\rm vd}\tau. \tag{82}$$

This is the pumping rate (in units of $\Gamma_{\rm vd}$) of atoms with resonant absorption frequencies that were Doppler shifted to the center of the spectral profile of the pumping light. The characteristic intensity I_p is the light intensity required to make $p = 1$. Values of p on the order of 1 or greater are needed to impart high spin polarization to an atom before a velocity-changing collision shifts the atomic absorption frequency out of resonance with the pumping light. The factor $\Gamma_{\rm vd}\tau$ that occurs in the definition (82) of I_p is normally much smaller than 1. For example for a representative rate of velocity-changing collisions $\Gamma_{\rm vd} = 2 \times 10^4\ {\rm s}^{-1}$ and $\tau = 16.23$ ns, we will have $\Gamma_{\rm vd}\tau = 3.2 \times 10^{-4}$. This means that light intensities large enough to cause many photon scattering cycles in the time intervals between velocity changing collisions can be far below optical saturation intensities I_s, which will cause populations of excited atoms comparable to those of ground-state atoms.

With these dimensionless quantities, Eq. (68) has the form of Eq. (1)

$$\frac{\partial}{\partial t}\Phi_k = -K_{r_k}\Phi_k + S_k. \tag{83}$$

The damping operator K_{r_k} for weak collisions is

$$K_{r_k} = -\frac{1}{2}\frac{\partial^2}{\partial x^2} - \frac{\partial}{\partial x}x + r_k, \tag{84}$$

where the dimensionless damping rate of the mode k is

$$r_k = \frac{\gamma_k}{\Gamma_{\rm vd}}. \tag{85}$$

In 1891, Rayleigh [15] wrote down Eq. (83) and its impulse-response function (4)

$$(x|T_r(\tau)|x') = \frac{e^{-r\tau}}{\sqrt{\pi(1-e^{-2\tau})}} \exp\left\{-\frac{(x - x'e^{-\tau})^2}{1-e^{-2\tau}}\right\}, \tag{86}$$

which one can verify by substitution into Eq. (83). This is the earliest mention of these important equations that we know of. Rayleigh's interest was the same as ours, the evolution of velocity distributions due to weak collisions. In 1916 Smoluchowski, apparently unaware of Rayleigh's earlier work, also stressed the importance of Eqs. (83) and (86)—see Eqs. (50) and (51) on pages 93 and 94 of Ref. [16]. There were many subsequent discussions of these equations, for example in 1930 by Uhlenbeck and Ornstein [17] and by other more recent authors. Equation (83) with $S_k = 0$ is one of the simplest Fokker-Planck equations. A clear summary of Fokker-Planck physics can be found in Risken's book, *The Fokker-Planck Equation* [18].

The dimensionless source rate for the mode k of Eq. (83) is

$$S_k = (\!(\gamma_k|S)\!) = -pg\sum_{l=1}^{m} C_{kl}\Phi_l, \tag{87}$$

where the mode coupling matrix is

$$C_{kl} = (\!(\gamma_k|A_{\rm op}|\gamma_l)\!) \quad \text{or} \quad A_{\rm op} = \sum_{lk} |\gamma_l) C_{lk} (\!(\gamma_k|. \tag{88}$$

Representative mode-coupling matrices for D_1 light propagating along the z and x axes, with optical pumping matrices (55) and (63), are

$$C(\mathbf{z}) = \frac{1}{3}\begin{bmatrix} 0 & 0 & 0 & 0 \\ -2 & 2 & 0 & 0 \\ 0 & 0 & 3 & 0 \\ 0 & 0 & 0 & 3 \end{bmatrix}, \quad \text{and} \quad C(\mathbf{x}) = \frac{1}{6}\begin{bmatrix} 0 & 0 & 0 & 0 \\ 0 & 6 & 0 & 0 \\ -2 & 0 & 5 & -1 \\ -2 & 0 & -1 & 5 \end{bmatrix}. \tag{89}$$

From Eq. (89) we see that

$$C_{1j} = 0. \tag{90}$$

Equation (90) is true, in general, since it expresses the fact that atoms are neither created nor destroyed by optical pumping.

From Eq. (3) we see that the solution to Eq. (83) is

$$\Phi_k(x,t) = \int_0^\infty d\tau \int_{-\infty}^{\infty} dx'(x|T_{r_k}(\tau)|x')S_k(x', t-\tau). \tag{91}$$

For pumping with unmodulated light, atoms will quickly reach a steady state with time-independent amplitudes, given for $k = 2, 3, \ldots, m$ by Eq. (5) as

$$\Phi_k(x) = \int_{-\infty}^{\infty} (x|G_{r_k}|x')S_k(x')dx'. \tag{92}$$

Integrating Eq. (92) over all relative velocities x and using the area theorem (136) with Eq. (87) we find, for $k = 2, 3, \ldots, m$,

$$\int \Phi_k(x)dx + \frac{p}{r_k}\sum_{l=1}^{m} C_{kl}\int g(x)\Phi_l(x)dx = 0. \tag{93}$$

The identity (93), valid for weak or strong collisions, is useful for checking numerical work.

For $k = 1$ and $r_k = 0$ the amplitude is the dimensionless version of Eq. (33)

$$\Phi_1 = \frac{e^{-x^2}}{\sqrt{\pi}}. \tag{94}$$

Substituting Eq. (87) into Eq. (92) we find the coupled integral equations for $k = 2, 3, \ldots, m$

$$\sum_{l=2}^{m}\int (x|V_{kl}|x')\Phi_l(x')dx' = F_k(x). \tag{95}$$

This is a (vector) Volterra equation with the kernel

$$(x|V_{kl}|x') = \delta_{kl}\delta(x-x') + pC_{kl}(x|G_{r_k}|x')g(x'), \tag{96}$$

and with the source

$$F_k(x) = -pC_{k1}\int (x|G_{r_k}|x')g(x')\Phi_1(x')dx'. \quad (97)$$

If we represent the mode amplitudes $\Phi_k(x)$ as vectors with n evenly spaced sample points x_j in velocity space, then the Volterra equation (95) is simply a set of $n(m-1)$ simultaneous linear equations, which can readily be solved by modern computer software like MATLAB, even if there are hundreds of coupled equations.

Having found the mode amplitudes Φ_k from Eq. (94) and the solution of Eq. (95), we can write the full, velocity dependent density matrix, Eq. (80), as

$$|\Phi) = \tfrac{1}{2}|1^{\{g\}})\Phi_1 + |S_z)\Phi_2 + |S_-)\Phi_3 + |S_+)\Phi_4. \quad (98)$$

We can characterize the steady-state spin distributions with the velocity-dependent expectation values of $|\Phi)$

$$(1^{\{g\}}|\Phi) = \Phi_1, \quad (99)$$

$$(S_x|\Phi) = \frac{1}{2}(\Phi_3 + \Phi_4) = \mathrm{Re}(\Phi_3), \quad (100)$$

$$(S_y|\Phi) = \frac{1}{2i}(\Phi_3 - \Phi_4) = \mathrm{Im}(\Phi_3), \quad (101)$$

$$(S_z|\Phi) = \frac{1}{2}\Phi_2. \quad (102)$$

From Eq. (66) we see that the the photon absorption rate of atoms with velocities between v and $v + dv$ is

$$(\Gamma_{\mathrm{dp}}|\Phi) = \Gamma_{\mathrm{vd}}p\,g\{\Phi_1 - n_z\Phi_2 - 2n_x\mathrm{Re}(\Phi_3) - 2n_y\mathrm{Im}(\Phi_3)\}. \quad (103)$$

The total absorption per atom, Eq. (65), becomes

$$\langle\delta\Gamma\rangle = \Gamma_{\mathrm{vd}}p\{\langle\Phi_1\rangle - n_z\langle\Phi_2\rangle - 2n_x\mathrm{Re}\langle\Phi_3\rangle - 2n_y\mathrm{Im}\langle\Phi_3\rangle\}, \quad (104)$$

where the spectrally averaged mode amplitudes are

$$\langle\Phi_j\rangle = \int g\Phi_j dx. \quad (105)$$

III. EXAMPLES

The key mathematical tool for solving Eq. (95) is the Green's function G_r that is needed to construct both the kernel (96) and the source (97). Expansions of the Green's functions on Hermite polynomials H_n are given by Eq. (260) for strong collisions, or by Eq. (236) for weak collisions. In practice, these expansions converge slowly because the maximum spatial frequencies (for velocity space) associated with $H_n(x)$ are of order $\sqrt{n}$, unlike the familiar Fourier series, where the spatial frequencies of e^{inx}, the analog of $H_n(x)$, are n. So inconveniently large values of n are needed to represent rapid variations of $(x|G_r|x')$ with x or x'. Beterov *et al.* [19] used Eq. (6) with Eq. (86) for weak collisions to evaluate the Green's function $(x|G_{1/2}|x')$; they display some examples in their Fig. 2. In all of the examples of this section we used the closed-form Green's functions (263) for strong collisions, or Eq. (132) for weak collisions.

Representative polarizations generated by monochromatic pumping light and by nonmonochromatic light with a Gaussian spectral profile are shown in Figs. 2 through 5. These

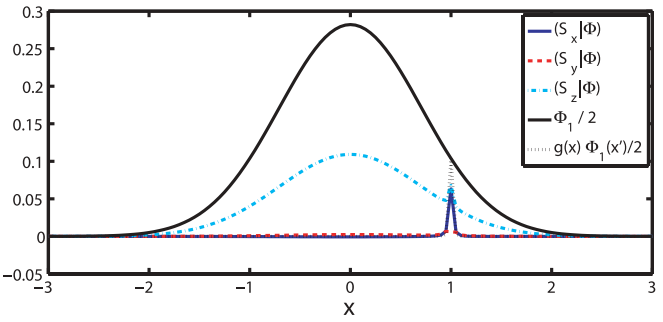

FIG. 2. (Color online) The spin polarization generated by monochromatic pumping light that excites a velocity group with $x_0 = 1$. The polarization is discontinuously transferred to all other velocity groups by strong collisions. The relative optical pumping rate is $p = 20$. The light propagates along the unit vector **n**, with Cartesian projections $[n_x, n_y, n_z] = [1, 0, 1]/\sqrt{2}$. The relative damping rate is $r = 0.01 + i$, that is, the atoms have a relatively small spin-damping rate $\Gamma_{\mathrm{sd}}/\Gamma_{\mathrm{vd}} = \mathrm{Re}\,(r) = 0.01$ and a relatively large Larmor frequency $\omega/\Gamma_{\mathrm{vd}} = \mathrm{Im}(r) = 1$, about the z axis. Because of the finite number, Eq. (121), of sample points along the x axis, the apparent widths of the lineshape function g and the resonant polarization amplitudes are exaggerated, and the amplitudes of the resonant polarization amplitudes are suppressed.

polarizations were calculated by direct solution of the Volterra equation (95), with 121 evenly spaced sample points along the x axis. For monochromatic light, this is not enough sample points to adequately represent narrow lineshape function g, and before using g in the numerical calculation (the solution of 121 simultaneous linear equations) we made the replacement

$$g_i \to \frac{g(x_i)\Delta x}{\int g(x)dx}. \quad (106)$$

Here $\int g(x)dx$ is the discrete approximation to the integral over g (we used the trapezoidal approximation). This ensures that the discrete approximation of the modified lineshape function (103) has the area $\Delta x = \Delta v/v_D$, which we evaluate analytically from Eq. (49). The discretized δ-function for the

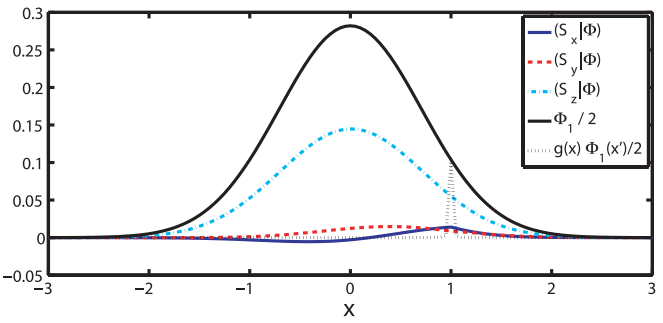

FIG. 3. (Color online) The spin polarization generated by monochromatic pumping light that excites a velocity group with $x_0 = 1$. The polarization is diffusively transferred to neighboring velocity groups by weak collisions. The parameters p, **n**, $\Gamma_{\mathrm{sd}}/\Gamma_{\mathrm{vd}}$, and $\omega/\Gamma_{\mathrm{vd}}$ have the same values as for Fig. 2. The longitudinal spin polarization has a Maxwellian velocity distribution and is similar to that for strong collisions, but the transverse polarizations are much larger and have a different, non-Maxwellian velocity distribution.

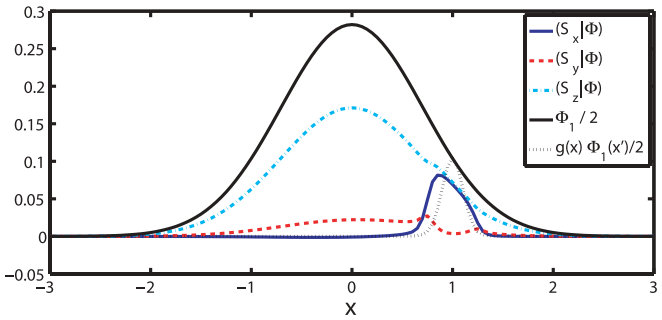

FIG. 4. (Color online) The spin polarization generated by pumping light with a Gaussian spectral profile for which the mean frequency excites a velocity group with $x_0 = 1$. The spectral profile g of the pumping light has a mean standard deviation $\sigma_x = 0.1$ in velocity space. The polarization is discontinuously transferred to all other velocity groups by strong collisions. The parameters p, $\mathbf{n}$, Γ_{sd}/Γ_{vd}, and ω/Γ_{vd} have the same values as for Fig. 2. The overall features are similar to the situation for monochromatic light shown in Fig. 2, but the sharp features for near-resonant velocities are smoothed out. Near the edges of the spectral profile, there is less suppression of $(S_y|\Phi)$, which is generated by precession of $(S_x|\Phi)$ around the z axis, by fast optical pumping in the x and z directions.

strong-collision Green's function (263) is $\delta(x - x') = \delta_{ij}/dx$ where $x = x_i$, $x' = x_j$ and $dx = x_2 - x_1$.

k. Alternate approach. For monochromatic pumping and weak collisions, there is a simpler approach that does not require a solution of the Volterra equation (95). Setting $g(x) = \Delta x \delta(x - x_0)$, where $\Delta x = \Delta v/v_D$ with v_D given by Eq. (79) and Δv by Eq. (50), we find from Eqs. (95) through (97) that

$$\Phi_k(x) = -p\Delta x(x|G_{r_k}|x_0)\sum_{l=2}^{m} C_{lk}\Phi_l(x_0), \quad \text{for} \quad k = 2, 3, \ldots, m. \tag{107}$$

So for monochromatic pumping at velocity x_0, the mode k has the same spatial dependence as the Green's function

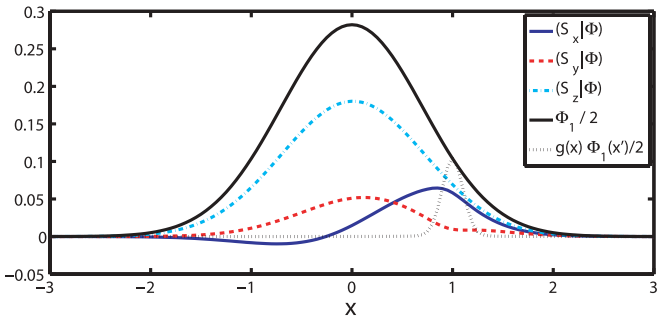

FIG. 5. (Color online) The spin polarization generated by pumping light with a Gaussian spectral profile for which the mean frequency excites a velocity group with $x_0 = 1$. The spectral profile g of the pumping light has a mean standard deviation $\sigma_x = 0.1$ in velocity space. The polarization is diffusively transferred to neighboring velocity groups by weak collisions. The parameters p, $\mathbf{n}$, Γ_{sd}/Γ_{vd}, and ω/Γ_{vd} have the same values as for Fig. 2. The overall features are similar to the situation for monochromatic light shown in Fig. 3, but the sharp features for near-resonant velocities are smoothed out.

$(x|G_{r_k}|x_0)$. Setting $x = x_0$ in Eq. (107), we see that the mode amplitudes $\Phi_k(x_0)$ are determined by the coupled linear equations

$$\sum_{k=2}^{m} M_{jk}\Phi_k(x_0) = N_j, \quad \text{for} \quad j = 2, 3, \ldots, m. \tag{108}$$

The elements of the $(m-1)\times(m-1)$ matrix M and the $(m-1)\times 1$ source vector follow from Eq. (107) and are

$$M_{jk} = \delta_{jk} + p\Delta x(x_0|G_{r_j}|x_0)C_{jk}, \quad \text{and} \quad N_j = -p\Delta x(x_0|G_{r_j}|x_0)C_{j1}\Phi_1(x_0). \tag{109}$$

The solution to Eq. (108) is

$$\Phi_k(x_0) = \sum_{j=2}^{m} M_{kj}^{-1}N_j. \tag{110}$$

Using Eq. (110) in Eq. (107) gives the complete solution to the problem. For weak collisions, polarizations calculated with this efficient alternative method cannot be distinguished from those obtained by solving the Volterra equation (95). For strong collisions the simple procedure outlined previously needs to be modified to give accurate results because of the δ functions that occur in the polarizations and in the Green's function (263).

A. White-light pumping

"White-light" pumping is a limiting case where the spectral profile of the light is equally intense for any velocity group. This will seldom be encountered for laser pumping, but optical pumping by sunlight will be of this type. We can assume that all polarization modes for white-light pumping have a Maxwellian velocity distribution so the mode amplitudes can be written as

$$\Phi_j = (\!(\gamma_j|\rho)\Phi_1. \tag{111}$$

The velocity-independent density matrix $\rho = \int \Phi dx$ was defined by Eq. (11). We will show that the assumption (111) is consistent with the Volterra equation (95).

We can let the pump lineshape function be velocity independent over the Maxwellian velocity distribution of Φ_1, and given by

$$g \to \bar{g} = 1. \tag{112}$$

Substituting Eqs. (111) and (112) into Eq. (95) and making use of the "weighted area theorem," Eq. (138), we find

$$r_k(\!(\gamma_k|\rho) = p\bar{g}\sum C_{kl}(\!(\gamma_l|\rho) = 0. \tag{113}$$

Multiplying Eq. (113) by $\sum_k |\gamma_k)$, and using Eqs. (69) and (88) we find

$$L|\rho) = 0, \tag{114}$$

where the net damping operator for polarized atoms with a Maxwellian velocity distribution is

$$L = \frac{i}{\hbar}H^{©} + \Gamma_{sd}A_{sd} + \bar{\Gamma}_{op}A_{op}. \tag{115}$$

Here the mean optical pumping rate is $\bar{\Gamma}_{op} = p\Gamma_{vd}/w$. We recognize Eq. (114) as the steady-state solution of the

conventional evolution equation for optical pumping

$$\frac{\partial}{\partial t}|\rho) = -L|\rho). \tag{116}$$

So for white-light pumping, the assumption (111) that all polarization amplitudes of the density matrix have the same Maxwellian distribution is valid. The density matrix is the solution of Eq. (116) if we are interested in transients, or the solution of Eq. (114) if we are interested in steady states. This happens for both strong or weak collisions and whether the relative damping rates r_j are large or small. This is not surprising, since a weak or strong velocity-changing collision moves the atom to a new velocity group, which experiences the same pumping rate from the "white light."

B. Fast v-Damping

For conventional laboratory experiments, where alkali-metal atoms are pumped in weakly depolarizing buffer gases, the rate of velocity-changing collisions is orders of magnitude faster than spin relaxation rates, and usually orders of magnitude faster that Larmor precession rates. In this case too, all polarization modes of the atom assume a Maxwellian velocity distribution, and as for white-light pumping, the mode amplitudes will be given by Eq. (111). Substituting Eq. (111) into Eqs. (95) through (97) and using the limiting expression (264) for $r_j \to 0$ we once again find Eq. (113), but with a mean pumping lineshape function

$$\bar{g} = \int \Phi_1 g\, dx = \langle \Phi_1 \rangle. \tag{117}$$

In the previous section we summarized how to solve Eq. (113).

In summary, for very fast v-damping, and with either strong or weak collisions, all of the polarization modes have Maxwellian distributions of velocity, just as in the case of white-light pumping. However, the reasons are very different. The light can have an arbitrary spectral profile g for very fast v-damping. The polarizations acquire a Maxwellian velocity distribution because of motional averaging in velocity space. Since $|r_j| = |\gamma_j|/\Gamma_{\rm vd} \ll 1$, the atom can be Doppler shifted into and out of resonance many times before there is appreciable spin relaxation, so the atom behaves as though it experiences a constant, velocity-averaged pumping rate.

IV. MATHEMATICS

We already alluded to the long history of this problem, which seems to have begun no later than Rayleigh's [15] work in 1891. The subsequent literature is scattered through various fields of physics, chemistry, and other disciplines. Some very useful results, like the closed-form expression (132) for the Green's function for weak collisions, seem not to be known. We therefore devote the remainder of this article to the mathematical tools that we found useful for analyzing problems like optical pumping of Na guidestar atoms. We begin by discussing weak collisions, where the damping operator K_r is given by Eq. (84), and for which the identity (6) can be written as

$$K_r G_r = \left(-\frac{1}{2}\frac{\partial^2}{\partial x^2} - \frac{\partial}{\partial x}x + r\right)(x|G_r|x') = \delta(x - x'). \tag{118}$$

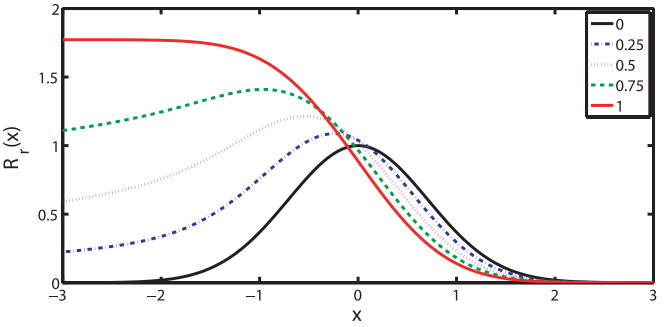

FIG. 6. (Color online) Representative functions $R_r(x)$. The relative damping rates r, of Eq. (118) have the values $r = 0,\ 0.25,\ 0.5,\ 0.75$, and 1. The function $R_r(x)$ is purely real when r is a real number.

To construct the Green's function with Eq. (118) we find "right" functions R_r, defined to within a normalizing factor by

$$K_r R_r = 0, \quad \text{with} \quad -\frac{1}{2}\frac{d}{dx}R_r - xR_r \to 0, \quad \text{as} \quad x \to \infty. \tag{119}$$

The boundary condition means that the current JR_r of Eq. (81) vanishes as quickly as possible as $x \to \infty$. Numerical values for the right functions can be found from the integral representation (149) or from the power series (164), which is particularly convenient for fairly small values of x. Examples of $R_r(x)$ are shown in Fig. 6 for representative real parameters r, and in Figs. 7 and 8 for representative imaginary values of r. Similarly, the left function L_r is defined by

$$K_r L_r = 0, \quad \text{with} \quad -\frac{1}{2}\frac{d}{dx}L_r - xL_r \to 0, \quad \text{as} \quad x \to -\infty. \tag{120}$$

For most values of r, L_r and R_r are linearly independent and it is possible to let

$$L_r(x) = R_r(-x). \tag{121}$$

The Wronskian for L_r and R_r is

$$W_r = L_r' R_r - L_r R_r', \tag{122}$$

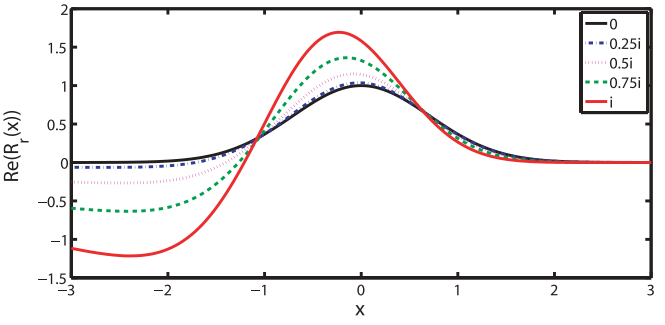

FIG. 7. (Color online) The real parts Re $(R_r(x))$, of the functions $R_r(x)$. The imaginary parts are shown in Fig. 8. The relative damping rates are $r = 0,\ 0.25i,\ 0.5i,\ 0.75i$, and i.

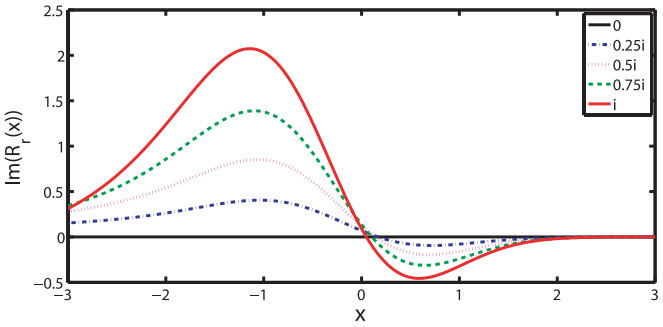

FIG. 8. (Color online) The imaginary parts of the functions $R_r(x)$, for which the real parts are shown in Fig. 7. The relative damping rates are $r = 0,\ 0.25i,\ 0.5i,\ 0.75i$, and i.

where

$$L_r' = \frac{dL_r}{dx} \quad \text{and} \quad R_r' = \frac{dR_r}{dx}. \tag{123}$$

Using Eqs. (119) and (120) we find that the Wronskian (122) satisfies the differential equation

$$\frac{dW_r}{dx} = -2xW_r. \tag{124}$$

The solution to Eq. (124) is

$$W_r(x) = W_r(0)e^{-x^2}. \tag{125}$$

The solutions L_r and R_r can be used to construct the Green's function defined by Eq. (132). We write the Green's function in terms of the left and right functions of the previous section as

$$(x|G_r|x') = \begin{cases} A(x')L_r(x) & \text{for} \quad x < x' \\ B(x')R_r(x) & \text{for} \quad x > x' \end{cases}. \tag{126}$$

To find the functions $A(x')$ and $B(x')$, we assume that the Green's function is continuous at $x = x'$, so we must have

$$A(x)L_r(x) - B(x)R_r(x) = 0. \tag{127}$$

If we integrate Eq. (118) over dx from $x = x' - \epsilon$ to $x = x' + \epsilon$, with ϵ being a small positive parameter we find

$$\begin{aligned} &-\frac{1}{2}\frac{\partial}{\partial x}(x|G_r|x')\bigg|_{x=x'+\epsilon} + \frac{1}{2}\frac{\partial}{\partial x}(x|G_r|x')\bigg|_{x=x'-\epsilon} \\ &+ r\int_{x'-\epsilon}^{x'+\epsilon}(x|G_r|x')dx - (x'+\epsilon)(x' \\ &+ \epsilon|G_r|x') + (x'-\epsilon)(x'-\epsilon|G_r|x') = 1. \end{aligned} \tag{128}$$

Using Eq. (126) in Eq. (128) and taking the limit for $\epsilon \to 0$ we find

$$A(x)L_r'(x) - B(x)R_r'(x) = 2. \tag{129}$$

Solving Eqs. (127) and (129) simultaneously we find

$$A = \frac{2R_r}{W_r}, \quad \text{and} \quad B = \frac{2L_r}{W_r}, \tag{130}$$

where the Wronskian was given by Eq. (122) or Eq. (125). Then Eq. (126) becomes

$$(x|G_r|x') = \frac{2L_r(x_<)R_r(x_>)}{W_r(x')}. \tag{131}$$

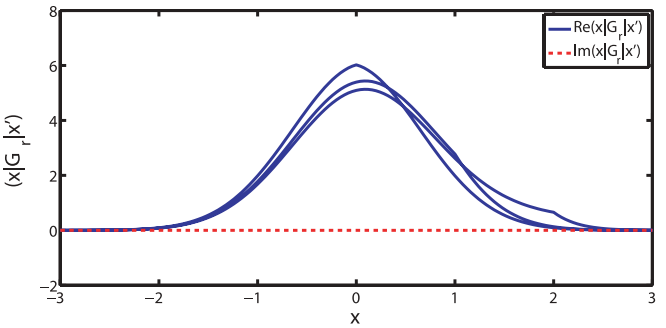

FIG. 9. (Color online) The Green's function $(x|G_r|x')$ of Eq. (132). The damping parameter is $r = 0.1$, corresponding to a situation where $\omega = 0$ and $\Gamma_{sd} = \Gamma_{vd}/10$. Polarized atoms are created at the dimensionless source velocities $x' = 0$, 1, and 2.

Finally, one can use Eqs. (121), (125), and (160) to write Eq. (131) as

$$(x|G_r|x') = \frac{2^r}{\sqrt{\pi}}\Gamma(r)e^{x'^2}R_r(-x_<)R_r(x_>). \tag{132}$$

Here $x_<$ is the lesser of x and x', and $x_>$ is the greater. The symbol $\Gamma(r)$ denotes the Euler Γ function (see Abramowitz and Stegun [20], Ch. 6) for the possibly complex damping rate r. Some representative Green's functions evaluated with Eq. (132) are shown in Figs. 9 through 11.

A. Areas

We define the "observation area" $I_r(x')$, of $(x|G_r|x')$ as the area of $(x|G_r|x')$ above the x axis. Using Eq. (131) we find

$$\begin{aligned} I_r(x') &= \int_{-\infty}^{\infty}(x|G_r|x')dx \\ &= \int_{-\infty}^{x'}(x|G_r|x')dx + \int_{x'}^{\infty}(x|G_r|x')dx \\ &= \frac{2R_r(x')}{W_r(x')}\int_{-\infty}^{x'}L_r(x)dx + \frac{2L_r(x')}{W_r(x')}\int_{x'}^{\infty}R_r(x)dx. \end{aligned} \tag{133}$$

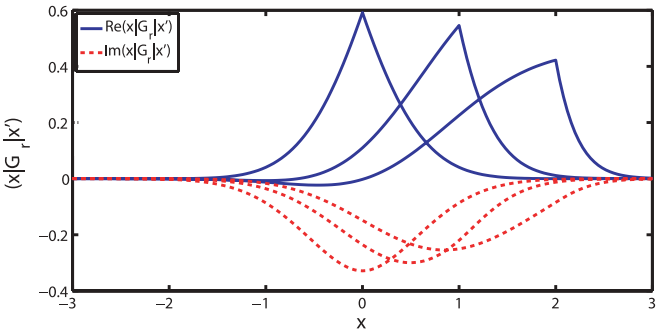

FIG. 10. (Color online) The Green's function $(x|G_r|x')$ of Eq. (132). The damping parameter is $r = 1 + i$, corresponding to a situation where $\Gamma_{sd} = \Gamma_{vd}$ and $\omega = \Gamma_{vd}$. Polarized atoms are created at the dimensionless source velocities $x' = 0$, 1, and 2.

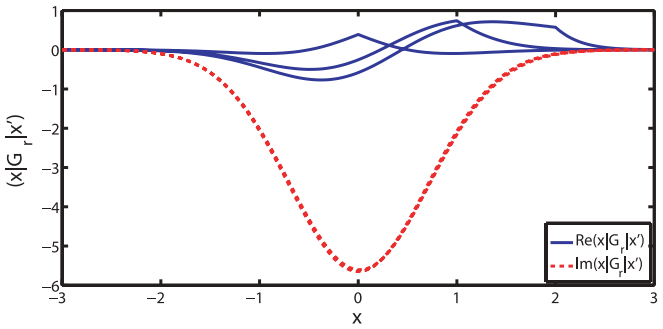

FIG. 11. (Color online) The Green's function $(x|G_r|x')$ of Eq. (132). The damping parameter is $r = 0.1i$, corresponding to a situation where $\omega = \Gamma_{vd}/10$, and $\Gamma_{sd} = 0$. Polarized atoms are created at the dimensionless source velocities $x' = 0$, 1, and 2.

Integrating Eq. (120) from $-\infty$ to x' we find

$$\int_{-\infty}^{x'} L_r(x)dx = \frac{1}{2r}[L_r'(x') + 2x'L_r(x')]. \tag{134}$$

Similarly, integrating Eq. (119) from x' to ∞ we find

$$\int_{x'}^{\infty} R_r(x)dx = -\frac{1}{2r}[R_r'(x') + 2x'R_r(x')]. \tag{135}$$

Substituting Eqs. (134) and (135) back into Eq. (133) we find

$$I_r(x') = \int_{-\infty}^{\infty}(x|G_r|x')dx = \frac{1}{r}. \tag{136}$$

The area is independent of the velocity x' at which the polarization is created.

We define the "weighted source area" by

$$\begin{aligned}\bar{I}_r(x) &= \int_{-\infty}^{\infty}(x|G_r|x')e^{-x'^2}dx' \\ &= \int_{-\infty}^{x}(x|G_r|x')e^{-x'^2}dx' + \int_{x}^{\infty}(x|G_r|x')e^{-x'^2}dx' \\ &= \frac{2R_r(x)}{W_r(0)}\int_{-\infty}^{x}L_r(x')dx' + \frac{2L_r(x)}{W_r(0)}\int_{x}^{\infty}R_r(x')dx'.\end{aligned} \tag{137}$$

Using Eqs. (134) and (135) in Eq. (137) we find

$$\bar{I}_r(x) = \int_{-\infty}^{\infty}(x|G_r|x')e^{-x'^2}dx' = \frac{e^{-x^2}}{r}. \tag{138}$$

Unlike the observation area I_r of Eq. (136) that depends only on r, the weighted source area, $\bar{I}_r(x)$, of Eq. (138) depends on both r and x.

Although derived previously for weak collisions, where the Green's function is given by Eq. (131), exactly the same area formulas, Eqs. (136) and (138), are found for the Green's function, Eq. (263), of strong collisions.

B. Contour Integrals for R_r

Following the methods outlined in the Mathematical Appendix of Landau and Lifschitz's, *Quantum Mechanics* [21], we assume that we can write the solution to Eq. (119) as the Laplace transform,

$$R_r = \int_C Ve^{xs}ds. \tag{139}$$

Here C is a contour in the complex s plane that begins at an initial point $s = s_i$ and ends at a final point $s = s_f$. The contour is independent of x. The integrand $V = V(s)$ is a function of s that is independent of x, but which may depend on the complex parameter r. We will choose the contour C to ensure that the function (139) satisfies the boundary condition of Eq. (119).

Substituting Eq. (139) into Eq. (119) we find

$$\int_C [P + xQ]Ve^{xs}ds = 0. \tag{140}$$

The functions P and Q are

$$P = 2(1-r) + s^2, \quad \text{and} \quad Q = 2s. \tag{141}$$

Integrating Eq. (140) by parts we find

$$[QVe^{xs}]_{s_f} - [QVe^{xs}]_{s_i} + \int_C [PVds - d(QV)]e^{xs}ds = 0. \tag{142}$$

This will be valid if the following two criteria are satisfied:

1. The value of the function QVe^{xs} is the same at the initial point s_i and the final point s_f of the contour C, so the first two terms of Eq. (142) cancel;
2. The third term of Eq. (142) is zero, which will be true if

$$PVds - d(QV) = 0, \quad \text{or} \quad V = \frac{N_r}{Q}\exp\left(\int\frac{P}{Q}ds\right). \tag{143}$$

For reasons that will become apparent in the following we will take the constant of integration to be

$$N_r = \frac{i}{\sqrt{\pi}(-1)^r}. \tag{144}$$

Using the values of P and Q from Eq. (141) in Eq. (143) we find

$$V = \frac{N_r e^{s^2/4}}{2s^r}. \tag{145}$$

Substituting Eq. (145) into Eq. (139) we find

$$R_r = \frac{i}{2\sqrt{\pi}}\int_C \frac{e^{xs+s^2/4}ds}{(-s)^r}. \tag{146}$$

The function

$$QVe^{xs} = \frac{N_r e^{s^2/4}}{s^{r-1}}, \tag{147}$$

must have the same value at both end points s_i and s_f of the contour C. Unless r is an integer, the function (147) is multiple valued; it has a branch point at $s = 0$. As we shall presently show, we can make Eq. (146) represent the right function R_r if we choose the contour C to be a vertical line in the complex s plane, between initial and final points

$$s_i = a + i\infty, \quad \text{and} \quad s_f = a - i\infty. \tag{148}$$

Here a can be any negative real number. This ensures that the contour C passes by the singularity at $s = 0$ on the left. Making

the substitution $s = -2iu - 2x$, in Eq. (146), we obtain

$$R_r(x) = \frac{e^{-x^2}}{\sqrt{\pi}} \int_{-\infty}^{\infty} \frac{e^{-u^2}}{(2x + 2iu)^r} du. \tag{149}$$

Here the path of integration is parallel to the real axis of the complex u plane and below the singularity at $u = ix$. Equation (149) is convenient for numerical evaluation of $R_r(x)$. For $r = 0$ one can readily find from Eq. (149) or from Eq. (146) that

$$R_0(x) = e^{-x^2}. \tag{150}$$

l. Formulas for: dR_r/dx; JR_r; xR_r. Differentiating Eq. (146) with respect to x and using the normalization coefficient (144) we find

$$-\frac{d}{dx} R_r = R_{r-1}. \tag{151}$$

Similarly, multiplying Eq. (146) by x, integrating by parts and using Eq. (144) we find

$$xR_r = \tfrac{1}{2} R_{r-1} - rR_{r+1}. \tag{152}$$

Combining Eqs. (151) and (152) we obtain

$$JR_r = rR_{r+1}, \tag{153}$$

where the current operator is given by Eq. (81). Integrating Eq. (151), we find

$$R_r(x) = \int_x^{\infty} R_{r-1}(u) du. \tag{154}$$

1. Values of $R_r(0)$, $W_r(0)$ and $(0|G_r|0)$

Recall that we can represent the inverse of Euler's Γ function—see Abramowitz and Stegun [20] **6.1.4**—with Hankel's contour

$$\frac{1}{\Gamma(z)} = \frac{i}{2\pi} \int_C \frac{e^{-t}}{(-t)^z} dt. \tag{155}$$

Here the path of integration C starts at $+\infty$ on the real axis of the complex t plane, encircles the origin in a counterclockwise direction, and returns to $+\infty$. Setting $x = 0$ in Eq. (146), making the substitution $s^2/4 = -t$, and using Eq. (155) we find

$$R_r(0) = \frac{\sqrt{\pi}}{2^r \Gamma\left(\frac{1}{2} + \frac{r}{2}\right)}. \tag{156}$$

Setting $r \to r + 1$ and $x = 0$ in Eq. (154) we find

$$\int_0^{\infty} R_r dx = R_{r+1}(0). \tag{157}$$

Alternatively, if we take $x' = 0$ in Eq. (135) we find

$$\int_0^{\infty} R_r dx = -\frac{R_r'(0)}{2r}. \tag{158}$$

Equating Eq. (157) to Eq. (158) we find

$$R_r'(0) = -2rR_{r+1}(0), \quad \text{and} \quad L_r'(0) = 2rL_{r+1}(0). \tag{159}$$

From Eqs. (122), (156), and (159) we find

$$\begin{aligned} W_r(0) &= 2r[L_{r+1}(0)R_r(0) + L_r(0)R_{r+1}(0)] \\ &= 4rR_r(0)R_{r+1}(0) = \frac{2\pi r}{2^{2r}\Gamma(\frac{1}{2} + \frac{r}{2})\Gamma(1 + \frac{r}{2})} \\ &= \frac{2\sqrt{\pi}}{2^r \Gamma(r)}. \end{aligned} \tag{160}$$

In reducing the product of the two Γ functions in the denominator of Eq. (159) to a single Γ function, we used the Gauss multiplication formula (Legendre's formula) [20]. We can also use Eq. (131) with Eqs. (156) and (160) to write

$$(0|G_r|0) = \frac{\Gamma\left(\frac{r}{2}\right)}{2\Gamma\left(\frac{r}{2} + \frac{1}{2}\right)}. \tag{161}$$

2. Complex Conjugates

With the definition (149) one can verify that the complex conjugate of $R_r(x)$ is given by

$$[R_r(x)]^* = R_{r^*}(x^*). \tag{162}$$

From Eqs. (162) and (132) we can also verify that for real x and x'

$$(x|G_r|x')^* = (x|G_{r^*}|x'). \tag{163}$$

a. Power series for R_r. From inspection of Eqs. (146) or (149) we see that $R_r(z)$ is an entire function of z with no singularities in the finite part of the complex z plane. It can therefore be written as the power series, convergent for all finite z

$$\begin{aligned} R_r(z) &= \sum_{n=0}^{\infty} \frac{1}{n!} \frac{d^n R_r}{dz^n}(0) z^n = \sum_{n=0}^{\infty} \frac{(-1)^n}{n!} R_{r-n}(0) z^n \\ &= \sum_{n=0}^{\infty} \frac{\sqrt{\pi}(-z)^n}{n! 2^{r-n} \Gamma\left(\frac{1}{2} + \frac{r}{2} - \frac{n}{2}\right)}. \end{aligned} \tag{164}$$

We used Eqs. (151) and (156) in evaluating the explicit coefficients of the power series.

b. Asymptotic expressions for $R_r(x)$ *at large* $|x|$. We can use Eq. (149) to see that for $x \to \infty$, the asymptotic value of R_r for $x \to \infty$ along the real axis is

$$R_r \sim \frac{e^{-x^2}}{(2x)^r}, \quad \text{for} \quad x \gg 1, \tag{165}$$

so the function (149) satisfies the boundary condition of Eq. (119). The analogous asymptotic value of R_r for $x \to -\infty$ along the real axis is

$$R_r \sim \frac{\sqrt{\pi}}{\Gamma(r)} (-x)^{r-1}, \quad \text{for} \quad x \ll -1. \tag{166}$$

To derive Eq. (166), one can choose the integration contour for t in Eq. (149) to have the segments: (a) $-\infty \to 0$, (b) $0 \to ix + i\epsilon$, (c) a complete, counterclockwise circle of radius ϵ around the branch point at $t = ix$, (d) $ix + i\epsilon \to 0$, and (e) $0 \to \infty$. All of the segments except (c) are straight lines. For $x \to -\infty$ the contributions to the integral from (a) and (e) vanish. For $\epsilon \to 0$ and $r < 1$, the contribution from (c) vanishes. For $\epsilon \to 0$, and $x \to -\infty$, the remaining contributions (b) and (d) give Eq. (166). One can use the identity (151) to show that Eq. (166) is valid for $r \geqslant 1$.

c. Asymptotic expressions for R_r *and* G_r *at large* $|r|$. To evaluate the inverse Laplace transform or Eq. (208), we need to know asymptotic expressions for $R_r(x)$ and $(x|G_r|x')$ for $|r| \to \infty$. We will use the method of steepest descent to find

these expressions. We write Eq. (149) as

$$R_r(x) = \frac{e^{-x^2}}{\sqrt{\pi}} \int_{-\infty}^{\infty} e^{\lambda_r} du, \tag{167}$$

where the exponent is

$$\lambda_r = -u^2 - r \ln(2x + 2iu). \tag{168}$$

The rate of change of λ_r with u is

$$\frac{\partial \lambda_r}{\partial u} = -2u - \frac{ir}{x + iu}. \tag{169}$$

Solving Eq. (169) for $\partial \lambda_r / \partial u = 0$ we find the summit locations of the two "passes"

$$u_\pm = \frac{i}{2}(x \pm \sqrt{x^2 + 2r}). \tag{170}$$

Substituting Eq. (170) back into Eq. (168) we find that the value of the exponent at the lower summit is

$$\begin{aligned} \lambda_r(u_-) &= \frac{1}{2}[r - x\sqrt{x^2 + 2r} + x^2 - 2r \ln(\sqrt{x^2 + 2r} + x)] \\ &\sim \frac{1}{2}[r - r \ln 2r - 2x\sqrt{2r} + x^2], \quad \text{as} \quad r \to \infty. \end{aligned} \tag{171}$$

The rate of change of the exponent (168) at the lower summit is

$$\frac{\partial^2 \lambda_r}{\partial u^2}(u_-) = -2 - \frac{4r}{(x + \sqrt{x^2 + 2r})^2} \sim -4, \quad \text{as} \quad r \to \infty. \tag{172}$$

Then we can approximate the integral (167) by the maximum value of the integrand at the top summit, times the integral over a Gaussian function with unit amplitude at u_- and with a curvature consistent with Eq. (172)

$$R_r(x) \sim \frac{1}{\sqrt{\pi}} \exp[-x^2 + \lambda_r(u_-)] \int_{-\infty}^{\infty} \exp -2(u - u_-) du, \tag{173}$$

or

$$\begin{aligned} \ln R_r(x) &\sim \frac{1}{2}(r - r \ln 2r - \ln 2 - 2x\sqrt{2r} - x^2), \\ \text{with} \quad &(|\arg r| < \pi). \end{aligned} \tag{174}$$

Evaluating Eq. (132) with Eq. (174) and with Stirling's well-known asymptotic limit—see Abramowitz and Stegun [20] (**6.1.37**)—for the Γ function

$$\begin{aligned} \ln \Gamma(r) &\sim (r - 1/2) \ln r - r + \tfrac{1}{2} \ln 2\pi, \\ \text{with} \quad &(|\arg r| < \pi), \end{aligned} \tag{175}$$

we find the asymptotic expression,

$$\begin{aligned} \ln(x|G_r|x') &\sim \frac{1}{2}(x'^2 - x^2 - 2|x - x'|\sqrt{2r} - \ln 2r), \\ \text{with} \quad &(|\arg r| < \pi). \end{aligned} \tag{176}$$

For large values of $|r|$, for example, $|r| = 10$ and $|\arg r| < \pi$, one can hardly tell the difference between plots of the asymptotic expressions (174) or (176) and the exact expressions (149) and (132). Larger values of $|r|$ are needed for large values of $|x|$ or $|x'|$ for Eq. (176) to be a good approximation.

C. Integer *r*

The function R_r reduces to well-known functions for values of r that are positive or negative integers, or zero. We already mentioned that $R_0(x) = e^{-x^2}$ in Eq. (150). Using Eq. (154) with Eq. (150) we conclude that

$$R_1(x) = \int_x^{\infty} e^{-x^2} dx = \frac{\sqrt{\pi}}{2} \text{erfc}(x). \tag{177}$$

Generalizing Eqs. (177) and (154) we conclude that for $n = 0, 1, 2, 3, \ldots, \infty$

$$\begin{aligned} R_n(z) &= \frac{\sqrt{\pi}}{2}(\text{i}^{n-1}\text{erfc}z) = \frac{\sqrt{\pi}}{2}\text{erfc}_{n-1}(z), \\ \text{for} \quad &n = 0, 1, 2, 3 \ldots, \infty, \end{aligned} \tag{178}$$

where i^n erfc z is the "Repeated Integral of the Error Function," discussed in Section **7.2** of Abramowitz and Stegun [20]. In using the function, i^n erfc z, it is important not to interpret it as the product of the nth power of the imaginary number i, and the complementary error function, erfc z. As indicated in Eq. (178), some authors use the less ambiguous notation $\text{erfc}_n(x)$, and the less ambiguous name, "the repeated erfc integral."

Using the expression (149) for nonnegative integers $n = 0, 1, 2, \ldots$, we find,

$$R_{-n}(x) = e^{-x^2} H_n(x), \tag{179}$$

where

$$H_n(x) = \frac{1}{\sqrt{\pi}} \int_{-\infty}^{\infty} (2x + 2iu)^n e^{-u^2} du \tag{180}$$

is a Hermite polynomial [20], $H_0(x) = 1$, $H_1(x) = 2x$, and so on. To prove that the function $H_n(x)$ given by Eq. (180) is indeed a Hermite polynomial we note: Eq. (180) can be readily verified for $n = 0$ or $n = 1$; the polynomials are even or odd functions of x depending on whether n is even or odd; for even n the x-independent term is $(-1)^{n/2} n!/(n/2)!$ as for Hermite polynomials; differentiating Eq. (180) we find $dH_n(x)/dx = 2nH_{n-1}(x)$, a well-known identity for Hermite polynomials, from which we can prove Eq. (180) by induction. We will refer to the functions R_{-n} as the eigenfunctions of K_r. Noting that $K_r = K_0 + r$ we see that

$$K_r R_{-n}(x) = (K_{-n} + r + n) R_{-n} = (r + n) R_{-n}, \tag{181}$$

so the eigenvalues are $(r + n)$. The eigenfunctions R_{-n} have currents, $J R_{-n}$ that, according to Eq. (153), are identically zero for $n = 0$ or that vanish (for $n > 0$) as $x^{n-1} e^{-x^2}$ for $x \to \pm\infty$. For all other values of r, one can use Eqs. (166) and (153) to show that the current diverges as $(-x)^r$ for $x \ll -1$. It was known for a long time that the Hermite functions (179) are eigenfunctions of K_r, for example, see Snider [22] or Risken [18].

From Eq. (179) we see that $L_{-n}(x) = (-1)^n R_{-n}(x)$ and therefore L_{-n} is not independent of R_{-n} for $n = 0, 1, 2, 3, \ldots, \infty$. We can get a solution Q_{-n} of the equation $K_{-n} Q_{-n} = 0$ that is linearly independent of R_{-n} by using an appropriately revised contour for the Laplace transform (139). We write

$$A_{-n} = \frac{1}{i\sqrt{\pi}(-1)^r} \int_C s^n e^{xs + s^2/4} ds. \tag{182}$$

Here the contour C starts at the origin of the complex s plane and goes up the imaginary axis to infinity. The initial and final points of this contour are

$$s_i = 0, \quad \text{and} \quad s_f = i\infty. \tag{183}$$

The function (147) is zero for these values of s_i and s_f, as required for the validity of Eq. (139). With the substitution

$$s = ik, \tag{184}$$

Eq. (182) becomes

$$A_{-n}(x) = \frac{(-i)^n}{\sqrt{\pi}} \int_0^\infty k^n e^{ixk-k^2/4} dk = \left(-\frac{\partial}{\partial x}\right)^n A_0. \tag{185}$$

We write the function A_{-n} as the sum of real and imaginary parts

$$A_{-n}(x) = R_{-n}(x) + i\,Q_{-n}(x), \tag{186}$$

where it will turn out that the R_{-n} of Eq. (186) is identical to the right function R_{-n} that was defined by Eq. (149). Thought of as a Fourier integral on the "phasors" e^{ikx}, the function A_{-n} of Eq. (185) is seen to have nonzero Fourier amplitudes only for nonnegative frequencies $k > 0$. In the signal-processing literature, $A_{-n}(x)$ will therefore be called an "analytic" signal. Except for sign, the real and imaginary parts of A_{-n} will be Hilbert transforms of each other, for example,

$$Q_{-n}(x) = \int_{-\infty}^{\infty} (x|\mathcal{H}|x') R_{-n}(x') dx', \quad \text{with} \quad (x|\mathcal{H}|x') = \frac{\mathcal{P}}{\pi(x-x')}. \tag{187}$$

Here $\mathcal{P}$ denotes the Cauchy principal part. For $n = 0$, Eq. (185) becomes

$$A_0(x) = \frac{1}{\sqrt{\pi}} \int_0^\infty e^{ixk-k^2/4} dk = e^{-x^2} \text{erfc}(-ix) = w(x), \tag{188}$$

where $w(x)$ is the Faddeeva function, which we discuss in Sec. IV D. For real x,

$$\text{Re}[A_0(x)] = \text{Re}[w(x)] = e^{-x^2} = R_0(x), \tag{189}$$

in agreement with Eq. (186). Taking the real part of Eq. (185) with Re (A_0) given by Eq. (189) we find

$$R_{-n}(x) = \left(-\frac{\partial}{\partial x}\right)^n e^{-x^2} = H_n(x) e^{-x^2}, \tag{190}$$

in agreement with Eq. (179).

Differentiating Eq. (185) we find the analog of Eq. (151)

$$-\frac{d}{dx} A_{-n} = R_{-n-1}. \tag{191}$$

Similarly, the analog of Eq. (153) is

$$J A_{-n} = -\frac{i}{\sqrt{\pi}} \delta_{n0} - n A_{-n+1}, \tag{192}$$

where the current operator is given by Eq. (81). Combining Eqs. (191) and (192) we find the analog of Eq. (152)

$$x A_{-n} = \frac{i}{\sqrt{\pi}} \delta_{n0} + \frac{1}{2} A_{-n-1} + n A_{-n+1}. \tag{193}$$

Combining the well-known asymptotic expression for the Faddeeva function, $w(x) \sim i/(\sqrt{\pi} x)$ with Eq. (185), we find

$$A_{-n}(x) \sim \frac{in!}{\sqrt{\pi} x^{n+1}} \quad \text{or} \quad Q_{-n}(x) \sim \frac{n!}{\sqrt{\pi} x^{n+1}}. \tag{194}$$

For large $|x|$ the amplitude of the in-phase signal R_{-n} is negligibly small compared to that of the quadrature signal Q_{-n}, which falls off as the power law (194).

In summary, we see that the right functions $R_r(x) = (\sqrt{\pi}/2)\,\text{erfc}_{r-1}$ can be be thought of as defining a generalization of the repeated erfc integral, so that the subscript n of $\text{erfc}_n = (2/\sqrt{\pi}) R_{n+1}$ can be any finite complex number, $|n| < \infty$, and need not be restricted to $n = 0, 1, 2, 3, \ldots, \infty$. For the eigenvalues $r = -n$ with $n = 0, 1, 2, 3, \ldots, \infty$, where the right function, $R_{-n} = e^{-x^2} H_n(x)$ is no longer independent of the left function, $L_{-n}(x) = R_{-n}(-x)$, the second solution can be taken to be Eq. (187), the Hilbert transform, Q_{-n}, of R_{-n} – or the "quadrature signal."

D. The plasma dispersion and Faddeeva functions

Here we briefly summarize properties of the plasma dispersion function

$$Z(z) = \frac{1}{\sqrt{\pi}} \int_{-\infty}^{\infty} \frac{e^{-t^2} dt}{t - z} \quad \text{for} \quad \text{Im}(z) \geqslant 0. \tag{195}$$

The closely related Faddeeva function—see Abramowitz and Stegun [20] (**7.1.3**)—is defined by

$$w(z) = e^{-z^2} \text{erfc}(-iz) = \frac{1}{\sqrt{\pi}} \int_0^\infty e^{izu-u^2/4} du. \tag{196}$$

The definition (196) works for all finite z. The integral extends for $u = 0$ to $u = \infty$ along the positive real axis. The plasma-dispersion function is proportional to the Faddeeva function, so a more general definition of Z than Eq. (195), which only works for Im $(z) \geqslant 0$, is

$$Z(z) = i\sqrt{\pi}\, w(z). \tag{197}$$

The Faddeeva function can be evaluated with a convenient MATLAB code due to Wiedeman [23], so we use w rather than Z in our computer codes. We note that

$$Z(0) = i\sqrt{\pi}, \quad \text{and} \quad w(0) = 1. \tag{198}$$

The "areas" of the functions Z and w are

$$\int_C Z(z) dz = i\pi, \quad \text{and} \quad \int_C w(z) dz = \sqrt{\pi}. \tag{199}$$

The contour C extends along the real axis of the complex z plane from $z = -\infty$ to $z = +\infty$. For $|z| \gg 1$ the values of Z and w approach the asymptotic limits

$$Z(z) \sim -\frac{1}{z}, \quad \text{or} \quad w(z) \sim \frac{i}{z\sqrt{\pi}}, \quad \text{for} \quad |z| \gg 1. \tag{200}$$

E. Expansions on Hermite polynomials

Rayleigh's transient (86), the Green's function (132), and the damping operator (84) can be expanded on the eigenfunctions (179). To see this we take the conventional

Laplace transform of Eq. (1) with respect to time to find

$$s\hat{y}_r - y_r(x,0) = -K_r\hat{y}_r + \hat{S}_r, \quad \text{with} \quad \hat{y}_r = \hat{y}_r(x,s) = \int_0^\infty y_r(x,t)e^{-st}dt. \tag{201}$$

Assume that $S_r(x,t) = 0$ for $t \leqslant 0$ so we can write the Laplace transform of the source as

$$\hat{S}_r(x,s) = \int_0^\infty S_r(x,t)e^{-st}dt = \int_{-\infty}^\infty S_r(x,t)e^{-st}dt. \tag{202}$$

Assuming no initial polarization $y_r(x,0) = 0$, and noting that $K_r + s = K_{r+s}$, we see that Eq. (201) becomes

$$K_{r+s}\hat{y}_r = \hat{S}_r. \tag{203}$$

Equation (203) is the steady-state version of Eq. (1), for which the solution was given by Eq. (5) as

$$\hat{y}_r(x,s) = \int_{-\infty}^\infty dx'(x|G_{r+s}|x')\hat{S}_r(x',s). \tag{204}$$

Using Eq. (132) we find

$$(x|G_{r+s}|x') = \frac{2^{r+s}}{\sqrt{\pi}}\Gamma(r+s)e^{x'^2}R_{r+s}(-x_<)R_{r+s}(x_>). \tag{205}$$

Inverting the Laplace transform (204) to return to the time domain, and using Eq. (202), we find

$$y_r(x,t) = \frac{1}{2\pi i}\int_{a-i\infty}^{a+i\infty} ds\, e^{st}\int_{-\infty}^\infty dx'(x|G_{r+s}|x')\hat{S}_r(x',s) = \int_{-\infty}^\infty dx'\int_{-\infty}^\infty dt'(x|T_r(t-t')|x')S_r(x',t'). \tag{206}$$

In the first line of Eq. (206), the path of integration in the complex s plane is vertical and is a distance a (a real number) to the right of the imaginary axis of the complex s plane. The value of a must be big enough that all singularities of the integrand are to the left of the path of integration. As we shall show in the following, this requires that

$$\mathrm{Re}(a) > -\mathrm{Re}(r). \tag{207}$$

The impulse-response function is the time-dependent kernel

$$T_r(\tau) = \frac{1}{2\pi i}\int_{a-i\infty}^{a+i\infty} ds\, e^{s\tau}G_{r+s}. \tag{208}$$

We see from Eq. (205) that the function G_{r+s} of Eq. (208) contains the factor $\Gamma(r+s)$, which has poles at $s = -n-r$, where $n = 0, 1, 2, 3, \ldots, \infty$. The other s-dependent factors of the integrand, 2^{r+s}, $R_{r+s}(x_<)$, $R_{r+s}(x_>)$ are all entire functions of s with no poles in the finite part of the complex s plane, but with singularities at $s = \infty$. We evaluate the integral (208) by picking a large circular path of integration, centered on $s = a$. As one can see from the asymptotic limit (176), the integrand G_{r+s} of Eq. (208) approaches zero on this circular path except near the negative real axis, where we can ensure negligible values by making the path pass between adjacent poles of G_{r+s}. The vertical path of integration of Eq. (208), from $a - i\infty$ to $a + i\infty$, will cut the large circle twice. We can close the contour of integration for $\tau < 0$ by integrating around the half circle to the right. Since the contribution from the semicircular part of the path is zero, the closed contour integral will have the same value as the integral (208). There are no poles of the integrand in the closed contour, so Cauchy's residue theorem implies that $T_r(\tau) = 0$ for $\tau < 0$. For $\tau > 0$ we can close the contour by integrating around the half circle to the left. The contribution to the integral from the semicircular part of the path will approach zero as the circle radius approaches infinity. Then $T_r(x,x',\tau)$ will be equal to the sum of the residues inside the closed contour. Recall that $\epsilon\Gamma(-n+\epsilon) \to (-1)^n/n!$ as $\epsilon \to 0$, so we can write Eq. (208) as

$$(x|T_r(\tau)|x') = \sum_{n=0}^\infty \frac{(-1)^n e^{x'^2}R_{-n}(-x_<)R_{-n}(x_>)e^{-(n+r)\tau}}{2^n n!\sqrt{\pi}} = \sum_{n=0}^\infty \frac{e^{-x^2}H_n(x)H_n(x')e^{-(n+r)\tau}}{2^n n!\sqrt{\pi}}, \quad \text{for} \quad \tau > 0. \tag{209}$$

We used Eq. (179), and we noted that $H_n(-x) = (-1)^n H_n(x)$ to convert to a series over Hermite polynomials.

For $r = 0$, the eigenvalue expansion (209) was given by Eqs. (5.46) and (5.64) of Risken [18]. But since the right functions R_r are little known and play such a central role in our analysis, we thought it would be useful to include the alternate derivation of Eq. (209) from the Green's function G_r of Eq. (205). As pointed by Eq. (5.65) of Risken [18], one can sum the series (209) with the following identity, valid for $-1 < \mathrm{Re}\,(u) < 1$,

$$\sum_{n=0}^\infty \frac{H_n(x)H_n(y)u^n}{2^n n!} = \frac{1}{\sqrt{1-u^2}}\exp-\left\{\frac{u^2x^2 - 2uxy + u^2y^2}{1-u^2}\right\}, \tag{210}$$

to show that Eq. (209) is identical to Rayleigh's transient, Eq. (86). Equation (210) is a special case of of Eq. **49.6.1** from Hansen [24]. Using Eq. (209) with Eq. (6) we find

$$(x|G_r|x') = \sum_{n=0}^\infty \frac{e^{-x^2}H_n(x)H_n(x')}{2^n n!\sqrt{\pi}(n+r)}. \tag{211}$$

The series (209) and (211) converge rather slowly to their closed-form limits, Eqs. (86) and (132), which are more practical for numerical work.

Using the differential form (84) for K_r, one can readily verify that

$$K_r e^{-x^2}H_n(x) = (n+r)e^{-x^2}H_n(x). \tag{212}$$

Multiplying Eq. (211) on the left by K_r and using Eq. (212) we find

$$K_r(x|G_r|x') = \sum_{n=0}^\infty \frac{e^{-x^2}H_n(x)H_n(x'')}{2^n n!\sqrt{\pi}} = \delta(x-x''), \tag{213}$$

the well-known completeness property of Hermite functions, and one possible representation of Eq. (6).

Using Eq. (213) and any function $y(x)$ we can write

$$y(x) = \sum_{n=0}^\infty \frac{e^{-x^2}H_n(x)}{2^n n!\sqrt{\pi}}\int_{-\infty}^\infty dx'H_n(x')y(x'). \tag{214}$$

Multiplying Eq. (214) by K_r and using Eq. (212) we find

$$K_r y(x) = \sum_{n=0}^{\infty} \frac{(n+r)e^{-x^2} H_n(x)}{2^n n! \sqrt{\pi}} \int_{-\infty}^{\infty} dx' H_n(x') y(x'). \tag{215}$$

From inspection of Eq. (215) we see that instead of writing K_r as the differential operator (84) we can write it as the kernel

$$(x|K_r|x') = \sum_{n=0}^{\infty} \frac{(n+r)e^{-x^2} H_n(x) H_n(x')}{2^n n! \sqrt{\pi}}. \tag{216}$$

V. OPERATOR ALGEBRA

As one might surmise from the fact that the weak-collision physics discussed previously is equivalent to forced drift and diffusion of particles in a harmonic-oscillator well, many of the concepts that proved so useful for coherent states [25] of oscillators have analogs for the weak-collision problem. To see these analogies, we define an abstract right eigenvector $|n)$, of K_r by

$$K_r|n) = (n+r)|n), \quad \text{where} \quad (x|n) = R_{-n} = e^{-x^2} H_n(x). \tag{217}$$

In like manner, we can define an abstract left eigenvector

$$(\!(n|K_r = (\!(n|(n+r) \quad \text{where} \quad (\!(n|x) = \frac{H_n(x)}{2^n n! \sqrt{\pi}}. \tag{218}$$

Since K_r is not a Hermitian operator, the left eigenvector is not simply the Hermitian conjugate of the right eigenvector, $(\!(n|x) \neq (x|n)^*$, as is obvious from Eqs. (217) and (218). Instead, $(\!(n|x)$ is a polynomial eigenfunction of the transpose operator K_r^T

$$K_r^T (\!(n|x) = (n+r)(\!(n|x). \tag{219}$$

The transpose operator is

$$K_r^T = K_r^{\dagger *} = -\frac{1}{2}\frac{\partial^2}{\partial x^2} + x\frac{\partial}{\partial x} + r. \tag{220}$$

The basis vectors $|x)$ and $(x'| = |x')^\dagger$ for velocity space are normalized such that

$$(x'|x) = \delta(x' - x). \tag{221}$$

The left and right vectors are complete and orthonormal, that is,

$$\sum_{n=0}^{\infty} |n)(\!(n| = 1, \quad \text{and} \quad (\!(n|n') = \delta_{nn'}. \tag{222}$$

We can write Eqs. (154) and (153) as

$$-\frac{d}{dx}|n) = |n+1), \quad \text{and} \quad -J|n) = n|n-1), \tag{223}$$

where the current operator J was given by Eq. (81). In operator form, we can write Eq. (223) as

$$-\frac{d}{dx} = \sum_{n=0}^{\infty} |n+1)(\!(n|, \quad \text{and} \quad -J = \sum_{n=0}^{\infty} (n+1)|n)(\!(n+1|. \tag{224}$$

We see that the operators $-d/dx$ and $-J$ play a role analogous to that of raising and lower operators for spin states or oscillator states in ordinary quantum mechanics. Since we are dealing with non-Hermitian systems $-d/dx$ and $-J$ cannot be chosen to be Hermitian conjugates of each other. One can readily verify the commutation relation

$$\left[J, \frac{d}{dx}\right] = 1. \tag{225}$$

The damping operator is

$$K_r = \frac{d}{dx} J + r. \tag{226}$$

d. Coherent states. In analogy to the discussion of oscillators we will define coherent state $|\alpha\rangle$ as the solution of the eigenvalue equation

$$J|\alpha\rangle = \alpha|\alpha\rangle. \tag{227}$$

We use the completeness property (222) to write

$$|\alpha\rangle = \sum_{n=0}^{\infty} |n)(\!(n|\alpha\rangle. \tag{228}$$

Substituting Eq. (228) into Eq. (227) and using Eq. (223), we readily find that the coefficients are

$$(\!(n|\alpha\rangle = \frac{(-\alpha)^n}{n!}, \quad \text{assuming that} \quad (\!(0|\alpha\rangle = 1. \tag{229}$$

Substituting Eq. (229) back into Eq. (228) and summing the series we find that the coherent state is

$$|\alpha\rangle = \exp\left(\alpha \frac{d}{dx}\right)|0), \quad \text{or} \quad (x|\alpha\rangle = (x+\alpha|0) = e^{-(x+\alpha)^2}. \tag{230}$$

e. Time dependence of a coherent state. The coherent state $|\alpha\rangle$ is simply the Maxwellian distribution $|0\rangle$ shifted to be centered at $x = -\alpha$ in velocity space. Forced drift and diffusion, together with a velocity-independent damping rate r will cause the coherent state to change at the rate

$$\frac{d}{dt}|\alpha\rangle = -K_r|\alpha\rangle. \tag{231}$$

Substituting Eq. (228) into Eq. (231) and using Eq. (217), we readily see that if the coefficients have the value (229) at time $t = 0$, they will have the value

$$(\!(n|\alpha\rangle_t = \frac{(-\alpha e^{-t})^n}{n!} e^{-rt} \tag{232}$$

at time t, so that Eq. (230) becomes

$$|\alpha\rangle_t = e^{-rt} \exp\left(\alpha e^{-t} \frac{d}{dx}\right)|0), \quad \text{or}$$
$$(x|\alpha\rangle_t = e^{-rt}(x + \alpha e^{-t}|0\rangle = e^{-(x-\alpha e^{-t})^2 - rt}. \tag{233}$$

The centroid velocity, $\bar{x} = -\alpha e^{-t}$ of the coherent state decays exponentially from its initial value $\bar{x} = -\alpha$ at $t = 0$ to $\bar{x} = 0$ at late times. The distribution remains Gaussian with constant variance $\sigma^2 = 1/2$.

f. Fundamental operators. We can use the left and right eigenvectors of Eqs. (217) and (218) to write the fundamental operators as

$$K_r = \frac{d}{dx} J + r = \sum_{n=0}^{\infty} (n+r)|n)(\!(n|, \tag{234}$$

$$T_r(\tau) = e^{-K_r\tau} = \sum_{n=0}^{\infty} |n)\!(\!(n|e^{-(n+r)\tau}, \tag{235}$$

$$G_r = \frac{1}{K_r} = \sum_{n=0}^{\infty} \frac{|n)\!(\!(n|}{n+r}. \tag{236}$$

We see from Eq. (234) that the damping rate of the mode $|n)$ of velocity space has a contribution n from drift and diffusion and a contribution r from velocity-independent damping, for example, from collisional spin relaxation or Larmor precession. Large-n modes damp more quickly than small-n modes because it is easier for drift and diffusion to damp distributions that vary rapidly in velocity space than distributions that vary slowly. Drift and diffusion cause no damping at all of the lowest mode $(x|0)$ because diffusion is exactly canceled by drift.

As discussed by Risken [18], Sec. **5.5.1**, it is possible to transform the Fokker-Planck equation for a parabolic potential into the Schrödinger equation for a harmonic oscillator so that one can use left and right eigenvectors that are Hermitian conjugates of each other. The equivalent approach earlier, with left and right eigenvectors that are not Hermitian conjugate pairs, obviates the need for this transformation.

VI. KEILSON-STORER MODEL

The preceding discussion was focused on weak collisions, where the velocity change per collision is small compared to the thermal velocity v_D. Na has a mass of approximately 23 amu, so for experiments with a light gas like He with a mass of 4 amu per atom or H_2 with a mass of 2 amu per molecule, the weak-collision limit should be a very good approximation. However, the masses of Na collision partners in the upper atmosphere, N_2, O_2, and O, are approximately 28, 32, and 16 amu. One will expect that there will be many "head-on" collisions that change the velocity by an amount comparable to the thermal velocity and we will be dealing with a substantial fraction of strong collisions in the Na layer.

To describe strong collisions, we will use the convenient, phenomenological, Keilson-Storer (KS) model [26]. Starting with the work of Rautian and Sobel'man [9,27], the KS model was widely used to analyze related problems [7–9,19,27]. We will also discuss little-known expansions of the KS model as infinite series in Hermite polynomials. We write the KS kernel [26] in dimensionless units as

$$(x|K_r|x') = \frac{1}{1-\alpha}\{\delta(x-x') - (x|W|x')\} + r\delta(x-x'), \tag{237}$$

where

$$(x|W|x') = \frac{e^{(x-\alpha x')^2/\Delta x^2}}{\Delta x\sqrt{\pi}}, \quad \text{with} \quad \Delta x^2 = 1-\alpha^2. \tag{238}$$

The real parameter α, with $0 \leqslant \alpha < 1$ parameterizes the strength of the collision, with $\alpha \to 1$ giving the weak-collision limit—the same as the Fokker-Plank limit we discussed previously, and with $\alpha = 0$ giving the strong-collision limit. For $\alpha \to 1$, the distribution $(x|W|x')$ of final velocities x has a very narrow spread, $\Delta x \ll 1$, and the distribution centroid $\alpha x'$ is nearly the same as the initial velocity x'. For $\alpha = 0$, every collision creates a Maxwellian distribution of final velocities. Kolchenko *et al.* [28] used the descriptive term "memory" parameter for α, since α is the fraction of the initial velocity x' "remembered" by the final velocities x. The velocity independent damping rate r was given by Eq. (85).

Using Eq. (201) we find

$$(x|W|x') = \sum_{n=0}^{\infty} \frac{\alpha^n e^{-x^2} H_n(x) H_n(y) u^n}{2^n n!}, \tag{239}$$

or

$$W = \sum_{n=0}^{\infty} \alpha^n |n)\!(\!(n|. \tag{240}$$

We discussed the left and right eigenvectors, $(\!(n|$ and $|n)$ in connection with Eqs. (217) and (218). Using Eq. (239) we can write the KS kernel (237) as

$$K_r = \sum_{n=0}^{\infty} \left(r + \frac{1-\alpha^n}{1-\alpha}\right) |n)\!(\!(n|. \tag{241}$$

Taking matrix elements of Eq. (241) we find

$$(x|K_r|x') = \sum_{n=0}^{\infty} \left(r + \frac{1-\alpha^n}{1-\alpha}\right) \frac{e^{-x^2} H_n(x) H_n(x')}{2^n n!\sqrt{\pi}}. \tag{242}$$

Exponentiating the kernel K_r of Eq. (241) to get the impulse-response function of Eq. (4) we find

$$T_r(\tau) = \sum_{n=0}^{\infty} e^{-[(r(1-\alpha)+1-\alpha^n]\tau'} |n)\!(\!(n|. \tag{243}$$

The time τ in units of the velocity damping time $1/\Gamma_{\rm vd}$ is related to the "dilated time," τ' by

$$\tau = (1-\alpha)\tau'. \tag{244}$$

Taking matrix elements of Eq. (243) we find

$$(x|T_r(\tau)|x') = \sum_{n=0}^{\infty} \frac{e^{-[(r(1-\alpha)+1-\alpha^n]\tau'} e^{-x^2} H_n(x) H_n(x')}{2^n n!\sqrt{\pi}}. \tag{245}$$

The expansion (245) of the KS impulse-response function as an infinite series in Hermite polynomials seems little known.

Inserting the power-series expansion, $e^{\alpha^n\tau} = \sum_q (\alpha^n\tau')^q/q!$, into Eq. (243) and changing the order of summation over n and q we find

$$T_r(\tau) = e^{-[(r(1-\alpha)+1]\tau'} \sum_{q=0}^{\infty} \frac{(\tau')^q}{q!} W_q, \tag{246}$$

where the partial kernels are

$$W_q = \sum_{n=0}^{\infty} \alpha^{qn} |n)\!(\!(n|. \tag{247}$$

A special case of Eq. (247) is $q = 0$ where the matrix elements of the partial kernel are

$$(x|W_0|x') = \delta(x-x'). \tag{248}$$

For $q \neq 0$ the matrix elements of the partial kernels are

$$(x|W_q|x') = \frac{e^{(x-\alpha^q x')^2/\Delta x_q^2}}{\Delta x_q \sqrt{\pi}}, \quad \text{where} \quad \Delta x_q^2 = 1 - \alpha^{2q}. \tag{249}$$

The partial kernels satisfy area identities reminiscent of Eqs. (136) and (138)

$$\int (x|W_q|x')dx = 1, \quad \text{and} \quad \int (x|W_q|x')e^{-x'^2}dx' = e^{-x^2}. \tag{250}$$

Taking matrix elements of Eq. (246) we find

$$(x|T_r(\tau)|x') = e^{-[(r(1-\alpha)+1]\tau'} \sum_{q=0}^{\infty} \frac{(\tau')^q}{q!}(x|W_q|x'). \tag{251}$$

With minor notational differences, the expression (251) of the impulse-response function as an infinite series of Gaussians was given by Keilson and Storer [7,26].

Taking the inverse of Eq. (241) in accordance with Eq. (6) we find the KS Green's function

$$G_r = \frac{1}{K_r} = \sum_{n=0}^{\infty} \frac{(1-\alpha)|n)(\!(n|}{r(1-\alpha)+1-\alpha^n}. \tag{252}$$

Taking matrix elements of Eq. (252) we write the KS Green's function as an infinite series of Hermite polynomials

$$(x|G_r|x') = \sum_{n=0}^{\infty} \frac{(1-\alpha)e^{-x^2}H_n(x)H_n(x')}{2^n n!\sqrt{\pi}[r(1-\alpha)+1-\alpha^n]}. \tag{253}$$

Alternately, we can use Eq. (251) with Eq. (6) to find the KS Green's function as an infinite series of Gaussians

$$(x|G_r|x') = \sum_{q=0}^{\infty} \frac{(1-\alpha)(x|W_q|x')}{[r(1-\alpha)+1]^{q+1}}. \tag{254}$$

In practice, Eqs. (253) or (254) must be truncated after a finite number of terms. For a given number of retained terms, the errors induced by truncation are comparable for the two series.

From inspection of Eq. (253) one can readily verify that the KS Green's functions have the same area identities, Eqs. (136) and (138), as the Fokker-Planck Green's functions

$$\int_{-\infty}^{\infty} (x|G_r|x')dx = \frac{1}{r}, \quad \text{and} \quad \int_{-\infty}^{\infty} (x|G_r|x')e^{-x'^2}dx' = \frac{e^{-x^2}}{r}. \tag{255}$$

The areas (255) are independent of α.

g. The limit $\alpha \to 1$. For the weak-collision limit of the KS model we write

$$\alpha = 1 - \epsilon, \quad \text{with} \quad \epsilon > 0. \tag{256}$$

Taking the limit of Eq. (241) as $\epsilon \to 0$,

$$\begin{aligned} K_r &= \lim_{\alpha\to 1} \sum_{n=0}^{\infty} \left(r + \frac{1-\alpha^n}{1-\alpha} \right) |n)(\!(n| \\ &= \lim_{\epsilon\to 0} \sum_{n=0}^{\infty} \left(r + \frac{1-(1-n\epsilon+\cdots)}{\epsilon} \right) |n)(\!(n| \\ &= \sum_{n=0}^{\infty} (r+n)|n)(\!(n|. \end{aligned} \tag{257}$$

This is the same as the expansion (234). For the limit $\alpha \to 1$ the KS model gives exactly the same results as the weak-collision model of forced diffusion in velocity space.

h. The limit $\alpha \to 0$. Taking the limit $\alpha \to 0$ in Eqs. (241), (245), and (252), and noting that $\alpha^0 = 1$ for all $\alpha > 0$ so $\alpha^0 \to 1$ as $\alpha \to 0$, we find the fundamental operators

$$K_r = \sum_{n=1}^{\infty} (1+r)|n)(\!(n| + r|0)(\!(0|, \tag{258}$$

$$T_r(\tau) = \sum_{n=1}^{\infty} |n)(\!(n|e^{-(1+r)\tau} + |0)(\!(0|e^{-r\tau}, \tag{259}$$

$$G_r = \sum_{n=1}^{\infty} \frac{|n)(\!(n|}{1+r} + \frac{|0)(\!(0|}{r}. \tag{260}$$

Noting that $(x|0) = e^{-x^2}$ and $(\!(0|x) = 1/\sqrt{\pi}$, we can use the completeness property (222) with (221) to find nonseries expressions for the matrix elements of Eqs. (258) through (260),

$$(x|K_r|x') = (1+r)\delta(x-x') - \frac{1}{\sqrt{\pi}}e^{-x^2}, \tag{261}$$

$$(x|T_r(\tau)|x') = e^{-r\tau}\left[\delta(x-x')e^{-\tau} + \frac{1}{\sqrt{\pi}}e^{-x^2}(1-e^{-\tau}) \right], \tag{262}$$

$$(x|G_r|x') = \frac{\delta(x-x')}{1+r} + \frac{e^{-x^2}}{r(1+r)\sqrt{\pi}}. \tag{263}$$

The damping operator (261) is the strong-collision version of the differential damping operator (84) for weak collisions, Eq. (262) is the strong-collision version of Rayleigh's transient (86), and Eq. (263) is the strong-collision version of the Green's function (132) for weak collisions.

i. The limit $r \to 0$. From inspection of Eqs. (236) and (252), we see that for both the Fokker-Planck model or for the KS model with any value of α the Green's functions approach the same limit as $r \to 0$,

$$(x|G_r|x') \to \frac{e^{-x^2}}{r\sqrt{\pi}}, \quad \text{as} \quad r \to 0. \tag{264}$$

If both the spin relaxation and spin-precession rates become very small compared to the rate of velocity-changing collisions, so $r \to 0$, a unit source at any velocity x' will build up a large polarization amplitude with a Maxwellian distribution of velocities x. Steady-state experiments for which r is known to be very small will not be sensitive to whether the velocity-changing collisions are weak or strong, since the limiting Green's function, Eq. (264), is the same in both cases.

VII. SUMMARY

We show how to calculate optical pumping phenomena in an unusual regime where: (a) the collision rates of optically pumped atoms with atoms or molecules of the background gas are small enough that individual velocity groups are preferentially excited, (b) the collision rates are still fast enough to partially transfer the spin polarization to other velocity groups, and (c) there are nonnegligible losses of polarization due to collisional spin relaxation and Larmor precession. This regime is similar to that of optically pumped

^{23}Na atoms of the Earth's upper atmosphere. But the conditions (a), (b), and (c) are seldom fulfilled at the same time in laboratory experiments with alkali-metal atoms. For example, in the work of Shimkaveg *et al.* [29] on optically pumped Li, at very low buffer-gas pressures, the conditions (a) and (b) were satisfied, but since the buffer gases of these experiments caused almost negligible spin relaxation and no transverse spin polarization was generated, there were negligible losses of spin polarization and condition (c) was not satisfied.

In Sec. II we show how to write the basic evolution equations in the Liouville space of the polarized atoms so that the evolution due to velocity-changing collisions at a rate $\Gamma_{\rm vd}$, Larmor precession at the frequency ω, collisional spin relaxation at the rate $\Gamma_{\rm sd}$, and optical pumping are clearly recognizable. We define weak collisions as those for which the velocity change in a single collision is very small compared to the mean thermal velocity v_D. In strong velocity-changing collisions the velocity change in a single collision is comparable to or larger than v_D. The fundamental evolution equation, Eq. (68), for weak collisions is a Fokker-Planck equation, apparently first written down by Rayleigh [15] in 1891. We show that for either weak or strong collisions, a simple and effective way to find the steady-state solution is with the Green's function $(x|G_r|x')$ that determines how much of the polarization generated by optical pumping at the "source" velocity $v' = x'v_D$ is transferred by collisions to the "observation" velocity $v = xv_D$. We assume that the polarization has a velocity-independent damping rate $\Gamma_{\rm sd} = r\Gamma_{\rm vd}$. The approach we outline is completely general and is applicable to real ^{23}Na atoms with nuclear spin quantum number $I = 3/2$. But to keep this article to a manageable length, we illustrated the key concepts with a simpler model: optical pumping, with circularly polarized D_1 light, of a hypothetical Na atom with $I = 0$.

In Sec. III we show examples of longitudinal and transverse spin polarization produced by optical pumping at low gas pressures and with strong or weak velocity-changing collisions. Whether the collisions are strong or weak makes little qualitative difference for longitudinal spin polarization, but the transverse spin polarization can be strikingly different for strong or weak collisions. We also show that, in the limit of white-light pumping or very fast velocity-changing collisions, all polarization components have Maxwellian velocity distributions.

We devoted about half of this article to the mathematical methods that we found most useful. In Sec. IV, which is devoted to weak collisions, we introduce "right functions," $R_r(x)$, of Eq. (149) from which we construct the Green's function G_r for weak collisions. The index r is normally a complex number with the real part representing a spin damping rate, and the imaginary part representing a spin-precession rate or Bohr frequency of some atomic coherence. The right functions $R_r(x)$ are entire functions of r or x (that is, with no poles for finite r or x). We show that for $-r = n$ with $n = 0, 1, 2, 3, \ldots, \infty$ the right functions are $R_{-n}(x) = H_n(x)e^{-x^2}$, where $H_n(x)$ is a Hermite polynomial.

In Sec. V we show that the right functions R_{-n} for $n = 0, 1, 2, \ldots$ can be used to construct right and left eigenvectors, $|n)$ and $(\!(n|$ of the damping kernel K_r and of the other fundamental operators $T_r(\tau)$ and G_r. The eigenfunctions are similar to those of a harmonic oscillator, perhaps not surprisingly, since the theory of weak collisions is that of diffusive motion in a parabolic potential well. Since we are discussing a dissipative, non-Hermitian system, the right and left eigenvectors are not simply Hermitian conjugates of each other. Introducing right and left eigenvectors allows one to analyze the effects of velocity-changing collisions with much the same algebraic methods as those that have become so familiar for coherent states of a harmonic oscillator [25].

Finally, in Sec. VI we show that the right and left eigenvectors for weak collisions are well suited for describing the KS model [26] of velocity-changing collisions. We give explicit expressions for the fundamental operators K_r, $T_r(\tau)$, and G_r for arbitrary values of the memory parameter α, and of the velocity-independent damping rate r. Weak collisions are modeled with $\alpha \to 1$, where the KS model and the Fokker-Planck model give identical results. Strong collisions are modeled with $\alpha = 0$.

ACKNOWLEDGMENTS

Special thanks are due Natalie Kostinski and Ivana Dimitrova for careful readings of this article and for many helpful suggestions. The authors wish to thank Edward Kibblewhite, Ronald Holzlöhner, and Paul Berman for useful discussions, and the Air Force Office of Scientific Research for support.

[1] W. Happer, G. J. MacDonald, C. E. Max, and F. J. Dyson, J. Opt. Soc. Am. A **11**, 263 (1994).
[2] P. W. Milonni, H. Fearn, J. M. Telle, and R. Q. Fugate, J. Opt. Soc. Am. A **16**, 2555 (1999).
[3] P. D. Hillman, J. D. Drummond, C. A. Denman, and R. Q. Fugate, Proc. SPIE **7015**, 70150L (2008).
[4] E. Kibblewhite, Proc. SPIE **7015**, 70150M (2008).
[5] R. Holzlöhner, D. B. Calia, and W. Hackenberg, Proc. SPIE **7015**, 701521 (2008).
[6] R. A. Bernheim, J. Chem. Phys. **36**, 135 (1962).
[7] E. Buhr and J. Mlynek, Phys. Rev. A **36**, 2684 (1987).
[8] P. R. Berman, *New Trends in Atomic Physics*, Les Houches Lecture Series (North-Holland, Amsterdam, 1984), p. 451.
[9] S. G. Rautian, Zh. Eksper. i Teor. Fiz. **51**, 1176 (1966) [Sov. Phys. JETP **24**, 788 (1967)].
[10] W. Happer, Y.-Y. Jau, and T. G. Walker, *Optically Pumped Atoms* (Wiley-VCH, Weinheim, 2010).
[11] R. R. Ernst, G. Bodenhausen, and A. Wokaun, *Principles of Nuclear Magnetic Resonance in One and Two Dimensions* (Oxford University Press, Oxford, England, 1990).
[12] W. Happer, Rev. Mod. Phys. **44**, 169 (1972).
[13] A. Einstein, Ann. Phys. (Leipzig) **17**, 549 (1905).
[14] G. P. M. Poppe and C. M. J. Wijers, ACM Trans. Math. Softw. **16**, 38 (1990).
[15] J. W. S. Rayleigh, *Scientific Papers* (Cambridge University Press, Cambridge, England, 1902), Vol. III, p. 473.

[16] S. Chandrasekhar, M. Kac, and R. Smoluchowski, *Marian Smoluchowski, His Life ad Scientific Work* (Polish Scientific Publishers, Warsaw, 2000).
[17] G. E. Uhlenbeck and L. S. Ornstein, Phys. Rev. **36**, 823 (1930).
[18] H. Risken, *The Fokker-Planck Equation. Methods of Solution and Applications* (Springer-Verlag, Berlin, 1989).
[19] I. M. Beterov, Y. A. Matyugin, S. G. Rautian, and V. P. Chebotaev, Zh. Eksp. Teor. Fiz. **58**, 1243 (1970) [Sov. Phys. JETP **31**, 668 (1970)].
[20] *Handbook of Mathematical Functions*, edited by M. Abramowitz and I. A. Stegun (Dover Publications, New York, NY, 1965).
[21] L. D. Landau and E. M. Lifschitz, *Quantum Mechanics: Non-Relativistic Theory* (Butterworth-Heinemann, Oxford, England, 1981), 3rd ed.
[22] R. F. Snider, Phys. Rev. A **33**, 178 (1986).
[23] J. A. C. Weidman, SIAM J. Numer. Anal. **31**, 1497 (1994).
[24] E. R. Hansen, *A Table of Series and Products* (Prentice-Hall, Englewood Cliffs, NJ, 1975).
[25] R. J. Glauber, Phys. Rev. **131**, 2766 (1963).
[26] J. Keilson and A. E. Storer, Q. Appl. Math. **10**, 243 (1952).
[27] S. G. Rautian and I. I. Sobel'man, Sov. Phys. Uspekhi **9**, 701 (1967).
[28] A. P. Kolchenko, A. A. Pukhov, S. G. Rautian, and A. M. Shalagin, Zh. Eksp. Teor. Fiz. **63**, 1173 (1972) [Sov. Phys. JETP **36**, 619 (1973)].
[29] G. Shimkaveg, W. W. Quivers, R. R. Dasari, and M. S. Feld, Phys. Rev. A **48**, 1409 (1993).